https://doi.org/10.5194/egusphere-2025-2135
Preprint. Discussion started: 18 June 2025


# Wind and Phytoplankton Dynamics Drive Seasonal and Short-Term Variability of Suspended Matter in a Tidal Basin

**Gaziza Konyssova[1,2*], Vera Sidorenko[1,2], Alexey Androsov[1,2], Sabine Horn[2], Sara Rubinetti[3], Ivan Kuznetsov[1], Karen Helen Wiltshire[2,4], Justus van Beusekom[2,5]**

[1] Alfred-Wegener-Institut Helmholtz-Zentrum für Polar- und Meeresforschung, Bremerhaven, Germany
[2] Wadden Sea Station Sylt, Alfred-Wegener-Institut Helmholtz-Zentrum für Polar- und Meeresforschung, List/Sylt, Germany
[3] Dipartimento per lo Sviluppo Sostenibile e la Transizione Ecologica, University of Piemonte Orientale, Vercelli, Italy
[4] Climate Science Trinity College Dublin, Dublin, Ireland
[5] Institute for Carbon Cycles, Helmholtz Centre Hereon, Geesthacht, Germany

*** Correspondence:**
Gaziza Konyssova
gaziza.konyssova@awi.de
ORCID: 0009-0008-5460-4754

**Abstract**

Suspended particulate matter (SPM) is a key component of coastal ecosystems, modulating light availability, nutrient transport, and food web dynamics. Its variability is driven by a combination of physical and biological processes that interact across temporal and spatial scales. Using the Sylt-Rømø Bight as a natural laboratory and focusing on the period 2000-2019, this study integrates a long-term biogeochemical time series from the Sylt Roads monitoring program and meteorological observations with Lagrangian transport simulations and neural network modelling to disentangle and quantify the relative roles of tidal dynamics, winds, and phytoplankton mediated biological processes in shaping SPM concentrations measured at two stations near the water surface.

The findings show that wind intensity dominates short-term SPM variability, particularly at the shallow station, where SPM responds rapidly to local wind-induced resuspension. At the deep station, the wind effects appear with a delay of ~5 days, aligning with tidally induced transport timescales (~133 hours) from shallower resuspension zones, as revealed by Lagrangian simulations. Seasonal patterns are further modulated by both reduced wind intensities and the onset of biological processes, with phytoplankton blooms promoting flocculation and subsequent settling in spring and summer. Neural network experiments highlight the shifting seasonal balance between physical and biological controls: models trained on winter data overestimate summer SPM levels by up to 80%, with only ~40% of this discrepancy explained by weaker winds and the remainder likely reflecting biologically mediated sinking processes.

https://doi.org/10.5194/egusphere-2025-2135
Preprint. Discussion started: 18 June 2025


## 1 Introduction

Suspended particulate matter (SPM) is a key component of coastal systems, influencing a wide range of physical and ecological processes. It consists of a mixture of small solid particles of both organic and inorganic origin suspended in the water column with concentrations, size (Eisma, 1986) and composition varying spatially and temporally (Schartau et al., 2019). The spatiotemporal variation in SPM levels is driven by an interplay of hydrodynamic, meteorological, and biological factors, which in turn, regulate nutrient availability, light penetration, and organic matter distribution. This directly impacts ecosystem productivity, including the timing of the phytoplankton bloom in spring (Cadée, 1986) and primary production gradients (Cloern, 1987; Colijn, 1982), and trophic interactions (Dolch and Reise, 2010; Graf and Rosenberg, 1997).

The focus of this study, the Sylt-Rømø Bight, is a tidally energetic basin within the Wadden Sea (southeastern North Sea), characterized by complex bathymetry and extensive intertidal flats. In such tidally energetic environments, the suspended matter gradient is kept upright by the density-driven coastward transport of bottom water and tidal straining (Becherer et al., 2016; Burchard et al., 2008; Flöser et al., 2011). The import of SPM and organic matter is reflected by the heterotropic nature of the Wadden Sea, where remineralisation of organic matter is larger than the local primary production (van Beusekom et al., 1999). Fine sediment accumulation in intertidal areas is further influenced by hydrodynamic retention mechanisms such as enhanced settling due to the landward dissipation of current velocity, the scour-lag (Dyer, 1995; Friedrichs and Aubrey, 1988) and settling lag effects (Postma, 1967), and the tidal asymmetry formed by the presence of non-linear processes within the tidal system (Dronkers, 1986; Fofonova et al., 2019; Friedrichs and Aubrey, 1988; Hagen et al., 2022). These processes collectively maintain coastal sediment balance and estuarine morphodynamics, contributing to the long-term evolution of tidal flat environments.

In addition to tidal-driven transport, wind stress and wave action are critical in short-term SPM variability. Wind-induced resuspension, particularly in shallow coastal areas, causes episodic increases in turbidity (Aarup, 2002). Stronger and more persistent wind forcing during winter maintains higher SPM levels, keeping fine sediments in suspension (de Jonge and van Beusekom, 1995; van Beusekom et al., 1999; Schubel, 1974), while calmer conditions in summer enable enhanced flocculation and settling (Bale et al., 1985; Fettweis et al., 2012).

Beyond physical transport mechanisms, SPM also interacts dynamically with a range of biogeochemical processes. It influences light penetration, nutrient availability, and food supply for suspension feeders (Cloern, 1987; Postma, 1981), while biological processes in turn regulate the aggregation, stabilization, and vertical flux of particulate matter (de Jonge and van Beusekom, 1995; van Beusekom and de Jonge, 2002; Fettweis and Van den Eynde, 2003). Flocculation—the aggregation of fine particles into larger, often organic-rich flocs—is a key mechanism by which biological activity modulates SPM concentrations (Wotton, 2004; Eisma, 1986). Natural flocs nearly always contain organic detritus, which may constitute anywhere from a minor to a dominant fraction of total floc mass (Engel and Schartau, 1999; Eisma, 1986), directly linking SPM dynamics to food-web functioning. The size and cohesiveness of these biologically mediated flocs also govern their settling velocities and resuspension thresholds, affecting how quickly particles are redistributed in the water column.

https://doi.org/10.5194/egusphere-2025-2135
Preprint. Discussion started: 18 June 2025


Benthic processes further influence SPM levels through both stabilization and removal mechanisms. While microphytobenthos, consisting of benthic diatoms and cyanobacteria, produce biofilms that stabilize sediments and reduce resuspension (Stal, 2010), filter-feeding organisms, such as mussels (*Mytilus edulis*) and oysters (*Magallana gigas*), alter SPM dynamics by removing fine particles from suspension, affecting both sediment deposition rates and nutrient cycling (Graf and Rosenberg, 1997). Moreover, excessive nutrient loads promote organic sedimentation, which alters benthic-pelagic coupling by influencing the availability of organic matter to both suspension and deposit feeders. The combination of wind-driven resuspension and strong tidal currents frequently elevates SPM concentrations, leading to fluctuating turbidity that can impact seagrass (*Zostera spp.*) productivity (Dolch and Reise, 2010).

Despite extensive research on hydrodynamic and wind-driven influences on SPM, their interaction with biological processes and relative contributions remain understudied. By leveraging long-term ecological monitoring data from the Sylt Roads program, this study aims to quantify the contributions of tidally induced and wind-driven resuspension and transport, as well as biologically mediated processes, to the spatiotemporal variability of SPM in the Sylt-Rømø Bight.

This analysis integrates high-resolution in situ measurements, meteorological data from the station List (Sylt, Germany), and outputs from hydrodynamic modelling to evaluate SPM dynamics across short-term (hourly to daily) and seasonal timescales. By using chlorophyll-a as a proxy for phytoplankton biomass, we approximate biological contributions triggered by phytoplankton to the variability of SPM levels, e.g. through flocculation and sediment stabilization. The study is guided by the following research questions: (1) What are the dominant mechanisms driving SPM variability across different temporal scales? (2) How do these mechanisms differ between the two monitoring stations within the Sylt-Rømø Bight?

## 2 Data and Methods

### 2.1 Area Description

The investigations were carried out in the Sylt Rømø Bight, a shallow, tidal basin in the northern Wadden Sea (southeastern North Sea; see Fig. 1). The basin is semi-enclosed due to two causeways at its northern and southern ends, isolating it from neighboring basins. Its only connection to the North Sea is through the deep tidal inlet Lister Deep, between the islands of Sylt and Rømø. The bay spans approximately 410 km² and features a highly variable topography, including extensive intertidal flats (>45%), shallow subtidal zones (~35%), and deep tidal channels (~10%). The Sylt-Rømø Bight's bathymetry is characterised by a mean water depth of approximately 4 m, with a maximum depth of about 37 m observed in the tidal inlet Lister Deep. Most subtidal and ~72% of intertidal sediments are sand-dominated.

The tidal range in the bight averages 2 m, based on observations at the List tide gauge (E.U. Copernicus Marine Service Information, doi.org/10.48670/moi-00036). Tidal forcing accounts for over 80% of depth-averaged velocity variability under regular wind conditions, in the absence of storms, and over 90% during spring tides (Fofonova et al., 2019). The bight receives minimal fluvial input, with small

https://doi.org/10.5194/egusphere-2025-2135
Preprint. Discussion started: 18 June 2025


rivers such as the Vidå and Brede Å (Fig.1), contributing only 4–10 $m^3/s$ of freshwater (Purkiani et al., 2015). Water exchange with the open North Sea occurs exclusively through Lister Deep, a 2.8 km wide tidal inlet. At the mouth of Lister Deep, a prominent ebb-tidal delta extends seaward, acting as both a sediment trap and a pathway for sediment redistribution within the bight (Dissanayake et al., 2012). A notable feature is Königshafen – a small shallow embayment at the northern tip of the island of Sylt. The embayment is sheltered from winds and waves, and experiences semidiurnal tides with amplitudes reaching 1.7 m (Kristensen et al., 2000; Reise and Siebert, 1994). With an average depth of ~2 m, large areas become exposed at low tide.

https://doi.org/10.5194/egusphere-2025-2135
Preprint. Discussion started: 18 June 2025


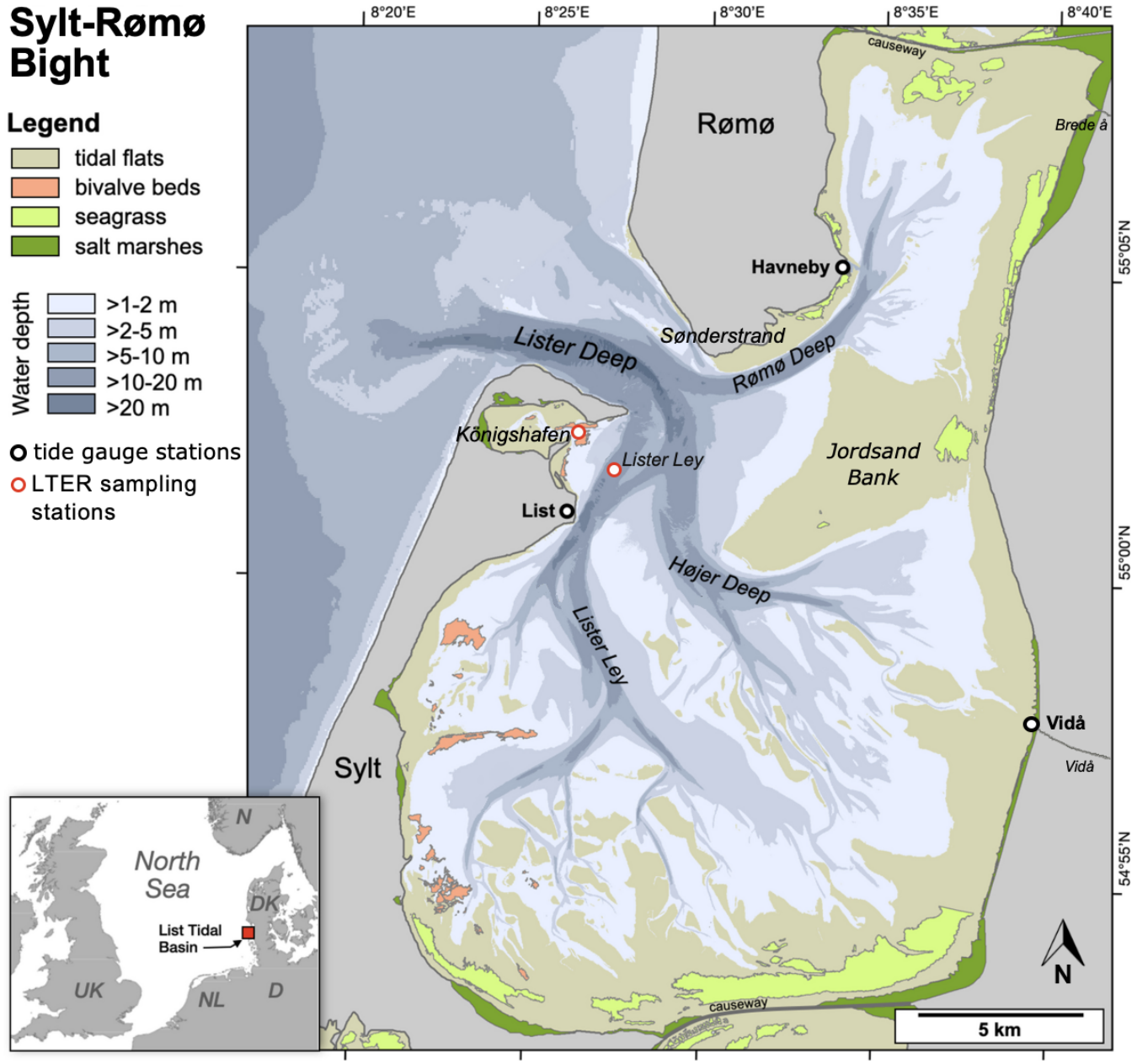


**Figure 1: Map of the Sylt-Rømø Bight showing bathymetry, key habitats (tidal flats, bivalve beds, seagrass meadows, and salt marshes), LTER sampling stations (Deep Station – Lister Ley; Shallow Station – Königshafen), tide gauge locations (List, Havneby, Vidå), and rivers (Brede Å and Vidå). The basin is connected to the North Sea via the tidal inlet Lister Deep and laterally enclosed by causeways to the north and south.**

## 2.2 FESOM-C Model

This study used the coastal hydrodynamic model FESOM-C (Androsov et al., 2019). FESOM-C is specifically designed for high-resolution coastal applications and employs a finite-volume cell-vertex

https://doi.org/10.5194/egusphere-2025-2135
Preprint. Discussion started: 18 June 2025


discretization on unstructured meshes composed of triangles and quadrilaterals. This allows for flexible spatial resolution down to several metres, suitable for simulating complex coastal dynamics (Fofonova et al., 2019; Kuznetsov et al., 2020, 2024; Neder et al., 2022; Sprong et al., 2020; Sidorenko et al., 2025).

### 2.2.1 Model Setup

The setup utilized an unstructured hybrid mesh of 208.345 nodes and 211.545 elements. Due to the semi-enclosed state of the bight, the mesh contains a single open boundary at the seaward edge of the domain, connecting the basin with the North Sea. The horizontal spatial resolution varies from up to 2 m in wetting-drying zones to 304 m in the deeper outer part (near the open boundary). The experiments were carried out by running 2D barotropic simulations with the wetting/drying option enabled to capture the periodic submergence and exposure of intertidal areas. The model timestep was set to ~ 0.25 seconds, with data output every ~20 minutes of simulation time. The bottom friction coefficient was applied as 0.0025, a value identified as optimal in prior studies of the same study area when using TPXO9 tidal solution (Fofonova et al., 2019, Konyssova et al., 2025).
The simulations are driven by tidal forcing alone, applied at the open boundary. For an accurate simulation of the tidal dynamics, the effects of higher harmonics and over-harmonics (e.g., Fofonova et al., 2019; Stanev et al., 2016) were taken into particular consideration as their role in shaping the hydrodynamics in such a shallow intertidal basin is significant. Therefore, thirteen major tidal harmonic constituents (M2, S2, N2, K2, K1, O1, P1, Q1, Mm, Mf, MN4, 2N, and S1) and two over-harmonics (M4, MS4) were prescribed by their phases and amplitudes at the open boundary based on TPXO9 tidal atlas (Egbert and Erofeeva, 2002). This selection of the tidal solution was justified by its robust performance and is one of the most optimal for the North Sea (Fofonova et al., 2019). The current setup has been validated in a previous work by Konyssova et al. (2025). The model's performance has been validated using tidal gauge (TG) data from stations List, Vidå, and Havneby, displayed in Fig. 1 (performance results are provided in the Supplementary Materials). Since the numerical setup remains unchanged, we refer to Konyssova et al. (2025) for full validation details.

### 2.2.2 Lagrangian Module

To assess tidally driven spatial connectivity and transport timescales within the basin, we performed Lagrangian simulations. These simulations were carried out using FESOM-C Drift, a post-processing tool designed for particle tracking. It simulates the movement of massless passive particles based on the velocity fields produced by the hydrodynamic model.
The experiment involved releasing passive tracers from all grid elements within the domain that are consistently inundated during every flood phase. We calculate about 90,000 tracers released every three hours over six weeks (169 iterations in total). Each tracer was tracked for up to three weeks and was removed from the simulation once it reached either of the two Sylt Roads sampling stations (see Fig. 1 and Section 2.3.1). Upon arrival at a station, tracers were immediately removed to prevent post-arrival movements from influencing the mapped source regions and transport pathways. The simulations were conducted independently for each station, focusing exclusively on the pathways from the release

https://doi.org/10.5194/egusphere-2025-2135
Preprint. Discussion started: 18 June 2025


locations to the respective sampling site. If a tracer did not reach the designated station within the simulation time frame, it was considered to originate from a region that falls outside the station's dominant transport pathways.

The first analysis approach assessed the source regions of passive tracers arriving at the sampling stations. This allows us to evaluate the connectivity between different subareas of the basin and the sampling sites. The probability of SPM originating from a given area was mapped based on the cumulative occurrence of tracer pathways across all iterations. Higher probability values indicate areas that more frequently serve as source regions or transport pathways for SPM reaching the sampling stations. The iterative release process was designed to capture the full range of tidal conditions and the complexity of hydrodynamic transport within the basin, ensuring that the results are statistically robust.

The second part of the analysis was conducted to estimate the mean transit time of the tracers reaching the sampling stations from shallow source zones, where resuspension typically occurs (defined here as areas <2 m deep, based on de Jonge & van Beusekom, 1995). The mean transit time over all implementations was calculated for all elements whose tracers reached the stations within the simulated three weeks. To quantify how long it typically takes for high tracer concentrations to reach the station, we computed a probability-weighted median transit time, where mean transit times were weighted by their probability values. This approach ensures that frequent transport pathways are given greater influence in the median transit time calculation, reducing bias from rare, low-probability trajectories.

## 2.3 Data

### 2.3.1 Biogeochemistry data

This study used data from the Sylt Roads long-term ecological monitoring program, focusing on a subset from 2000 to 2019 to ensure consistent methodology and regular sampling. From a broad range of hydrographic and biogeochemical parameters covered in the dataset, this study specifically analyzed suspended particulate matter (SPM; mg/L, filtered through 0.4 µm nucleopore filters, rinsed with distilled water, stored frozen, and dried at 60 °C) and chlorophyll-a (Chl-a; µg/L, filtered through GF/C filters (Whatman), stored at −20 °C, and extracted using 90% acetone). Both parameters were measured twice weekly at a sampling depth of 1 m below the surface at two primary stations: the deep station at the Lister Ley channel and the shallow station at the entrance of Königshafen embayment (see Fig. 1). The full dataset is publicly available on the data portal PANGAEA (https://www.pangaea.de) and the recent evaluation is detailed in Rick et al. (2023).

### 2.3.2 Meteorological data

For the statistical analysis, we also downloaded the quality checked historical meteorological data for station 3032, List auf Sylt, from Climate Data Center (CDC) of the Deutscher Wetterdienst (DWD). The data includes hourly mean wind speed and wind direction (dataset ID: urn:x-wmo:md:de.dwd.cdc::obsgermany-climate-hourly-wind), and daily sunshine duration (dataset ID: urn:wmo:md:de-dwd-cdc:obsgermany-climate-daily-kl). This product was available for download from https://opendata/dwd.de/climate_environment/, last access: 28 February 2025.

https://doi.org/10.5194/egusphere-2025-2135
Preprint. Discussion started: 18 June 2025


### 2.3.3 Sea Surface Height data

Using the validated model setup, the sea surface elevation (SSH) data was reconstructed for the deep and shallow stations. In particular, the amplitudes and phases of the 15 harmonics mentioned above were obtained from the modeling output using Fast Fourier Transform analysis. Subsequently, the SSH signal was reconstructed precisely for the observational time. The classical harmonic analysis routines from *t_tide* were utilized (Pawlowicz et al., 2002). The SSH data is then used to determine the tidal phases and elevation gradients when taking samples to include in the statistical and neural network (NN) analyses

**Table 1. The physical and hydrochemical parameters used in the study (short name, units, frequency, and source)**

| Data | Unit | Frequency | Source |
|---|---|---|---|
| SPM | mg/L | twice weekly | Sylt Roads Marine Observatory |
| Chl-a | µg/L | twice weekly | Sylt Roads Marine Observatory |
| Wind speed and direction | m/s, degrees | hourly mean | Deutscher Wetterdienst |
| Light | hours | daily | Deutscher Wetterdienst |
| SSH | m | every 20 minutes | Model reconstruction using 13 harmonics from tpx09 and verified with the tidal gauges |

## 2.4 Neural Network

To assess the relative contribution of biotic conditions to SPM concentrations, we employed a forward NN to predict SPM based on environmental input parameters. The approach relies solely on long-term observational data, which adds robustness to the results. Although numerical simulations are also powerful tools in this context, any discrepancies they produce can largely be attributed to the choice of numerical methods or the spatial and temporal resolution applied. An NN is particularly well-suited for this task, as it effectively captures complex, non-linear relationships between influencing factors. We conducted several sensitivity experiments (not shown), varying both the network depth and the number of neurons per layer. For the current application, increasing the network depth further did not improve performance.

The NN was implemented in several steps using a feedforward architecture with three hidden layers (e.g., Jain et al., 1996), consisting of 100, 40, and 20 neurons, respectively. Each neuron acts as a simple processing unit that transforms input into output using a mathematical function. In this case, we used a hyperbolic tangent (tanh) sigmoid transfer function, which maps input values into the range between –1 and 1 and enables the model to capture complex, non-linear relationships between environmental inputs and SPM concentrations. The output layer employed a linear activation function. The Levenberg–Marquardt algorithm is used as the learning function. For training, 60% of arbitrarily chosen SPM measurements were used, while the remaining data were split for validation and testing. A separate NN was developed for each station, and the datasets for different stations were not combined.

For the first part of the experiment, the primary regression task involved predicting SPM concentrations during the winter season, which is characterized by low biological activity, as indicated by minimal

https://doi.org/10.5194/egusphere-2025-2135
Preprint. Discussion started: 18 June 2025


Chl-a concentrations. Focusing on winter allows for a clearer assessment of physical (abiotic) drivers, such as wind forcing, with reduced biological confounding. The input feature, 21 in total, of the NN model includes wind magnitude at the time of sampling and averages over a series of prior time intervals (6 to 240 hours, corresponding to the intervals analyzed in Subsection 3.2.2), dominant wind direction over 6 and 12 hours (even though the correlation analysis shows only a minor impact, the non-linear effects of wind direction may still be present), salinity, current elevation, and the gradient of elevation (computed using a forward scheme). The results of the winter model are presented in Section 3.3.1.

To explore seasonal dynamics more comprehensively, we extended the model to include data from all seasons, first using the same input parameters as in the winter model (results in Section 3.3.3), and then incorporating two additional features: temperature and the weekly sum of sunshine hours prior to the measurement date (Section 3.3.4). The latter serves as a proxy for both Chl-a concentration and benthic algae abundance. In the shallow areas of the Sylt-Rømø Bight, light can reach the seafloor, stimulating benthic algae growth, provided water clarity allows sufficient light penetration (Loebl et al., 2007). This, in turn, helps stabilize sediments and reduce resuspension. Temperature plays a crucial role in regulating biological activity, including phytoplankton growth, bacterial metabolism, and production of extracellular polymeric substances (EPS). EPS, secreted by microorganisms, enhances particle aggregation by increasing stickiness and acting as a binding agent for fine sediments. Warmer temperatures also accelerate the decomposition of organic matter, influencing the availability of organic detritus that contributes to flocculation. In addition, temperature affects top-down controls such as zooplankton grazing, which alters SPM composition by consuming phytoplankton and restructuring organic aggregates. In this study, we do not attempt to separate these mechanisms individually but instead aim to highlight their combined influence on seasonal SPM variability.

## 3 Results

Figure 2 presents the time series of SPM concentrations at the deep and shallow stations in the Sylt-Rømø Bight from 2000 to 2019, based on data from the Sylt Roads monitoring program (Section 2.3.1; station locations shown in Fig. 1). Both stations display a pronounced seasonal cycle, with SPM concentrations typically peaking in winter and declining during summer. The deep station shows more frequent and sustained seasonal peaks in SPM levels throughout the time series, whereas the shallow station tends to exhibit higher concentrations during peak events. It is also important to note that the regular sampling at the shallow station was discontinued after 2013 following the replacement of the research vessel, resulting in reduced data coverage in subsequent years.

https://doi.org/10.5194/egusphere-2025-2135
Preprint. Discussion started: 18 June 2025


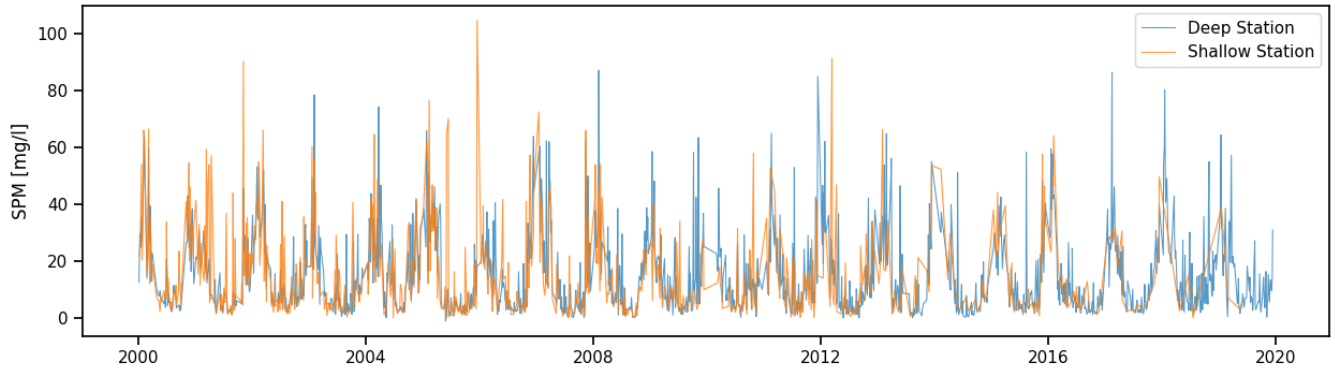


**Figure 2: Time series of SPM for the considered years (2000–2019) for the deep (blue) and shallow stations (orange).**

## 3.1 Seasonality of SPM concentrations

SPM concentrations show a clear seasonality with patterns reflecting the combined influence of biological activity and meteorological forcing. While various biological processes influence SPM dynamics, phytoplankton activity plays a particularly central role by triggering biologically mediated processes and directly contributing to flocculation and particle aggregation. For example, phytoplankton blooms in spring and summer can promote flocculation, leading to enhanced particle settling and reduced SPM concentrations in the water column (de Jonge & van Beusekom, 1995; Schartau et al., 2019). In contrast, stronger winds during winter enhance sediment resuspension, resulting in elevated SPM levels during the colder months. Using Chl-a as a proxy for phytoplankton biomass, this subsection examines how biological activity and wind forcing together shape seasonal patterns of SPM variability at both the deep and shallow stations.

### 3.1.1 Role of biological processes in seasonal SPM variations

Both stations exhibit distinct seasonal variations in SPM and Chl-a concentrations (Fig. 3). SPM levels are highest in late autumn and winter, on average 33.9 ± 18.2 mg/L at the deep and 38.6 ± 16.4 mg/L at the shallow stations and peaking in January at 63.5 ± 19.9 mg/L at the deep and 65.4 ± 18.3 mg/L at the shallow stations. The decline is observed through spring (February–May), reaching their lowest values in summer (June–August), averaging 2.5 ± 2.9 mg/L at both stations. From September onward, SPM begins to increase. This pattern is similar at both stations, though the shallow station generally has slightly higher SPM levels, suggesting potential differences in sediment availability or resuspension dynamics.

Chlorophyll-a concentrations follow an inverse seasonal pattern. Chl-a remains low in winter (2.1 ± 0.7 µg/L on average at both stations, December–January) and increases sharply in early spring, peaking between February and April before declining into summer. A secondary increase occurs in autumn (August–October). The deep station shows a more pronounced Chl-a peak (32.4 ± 18.1 µg/L) in early spring compared to the shallow station (25.0 ± 20.6 µg/L), though both stations exhibit a similar overall seasonal cycle.

https://doi.org/10.5194/egusphere-2025-2135
Preprint. Discussion started: 18 June 2025


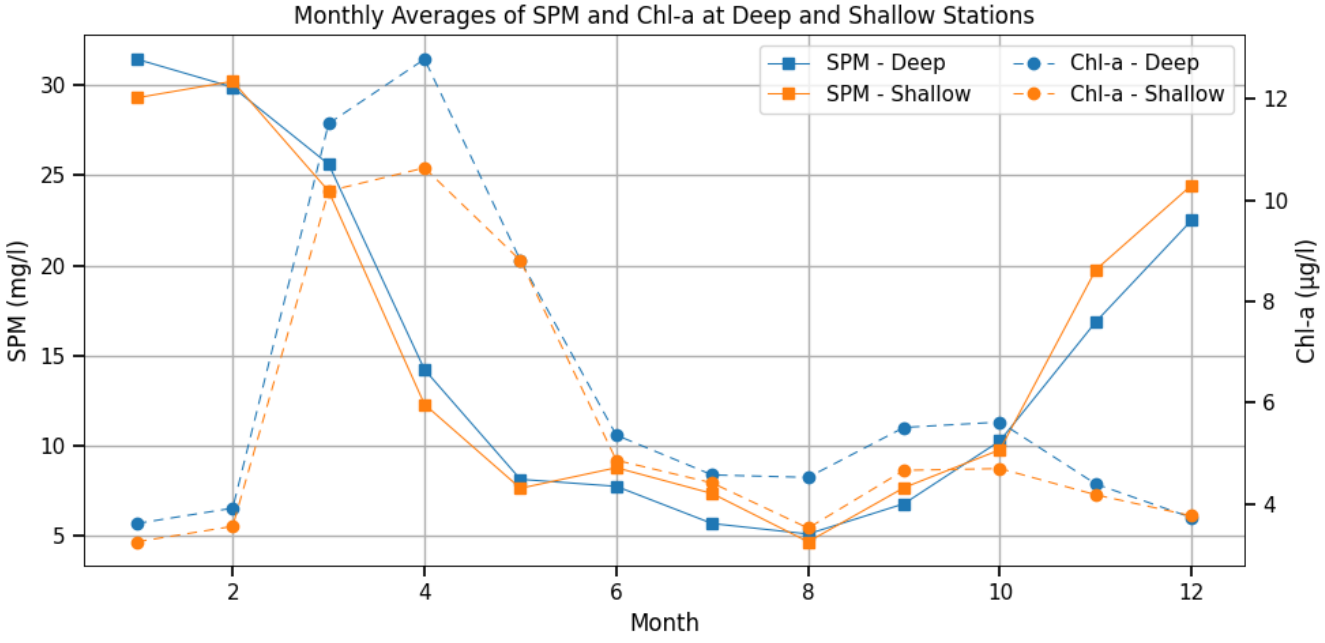


**Figure 3: Monthly averages of SPM and Chl-a at the deep (blue) and shallow (orange) stations for the considered years (2000–2019). SPM concentrations solid line with square marker, left axis) and Chl-a concentrations (dashed line with circle markers, right axis) are displayed separately for clarity. The x-axis represents the months from January to December.**

The relationship between Chl-a and SPM varies across seasons (Fig. 4), with the deep station generally having a weaker correlation than the shallow station. During winter months (December–February), when biological activity is low and Chl-a constitutes a relatively constant fraction of total SPM subject to the same resuspension processes, strong positive correlations are observed at both stations, with the highest values in December ($R^2 = 0.75$, shallow station) and January ($R^2 = 0.84$, deep station). The strong correlation and the slope is in line with the resuspension of microphytobenthos as observed in winter by de Jonge and van Beusekom (1995). From March onward, the relationship becomes more complex. As Chl-a rises rapidly during the spring bloom and SPM concentrations decline, the correlation at both stations weakens ($R^2 < 1$). This divergence reflects the dual role of phytoplankton: it contributes directly to SPM, yet also promotes aggregation and settling, thereby reducing suspended material. This non-linear and temporally variable influence of Chl-a also underlies the decision not to use it directly as a predictor in the neural network (Section 3.3), but instead to approximate biological activity through broader proxy variables. During summer (June–August), as both the SPM and Chl-a concentrations reach low values, the correlation weakens further, with August showing almost no correlation at the shallow station. In late autumn, particularly in November and December, the correlation strengthens again as the role of biological activity reduces and physical drivers become dominant again.

https://doi.org/10.5194/egusphere-2025-2135
Preprint. Discussion started: 18 June 2025


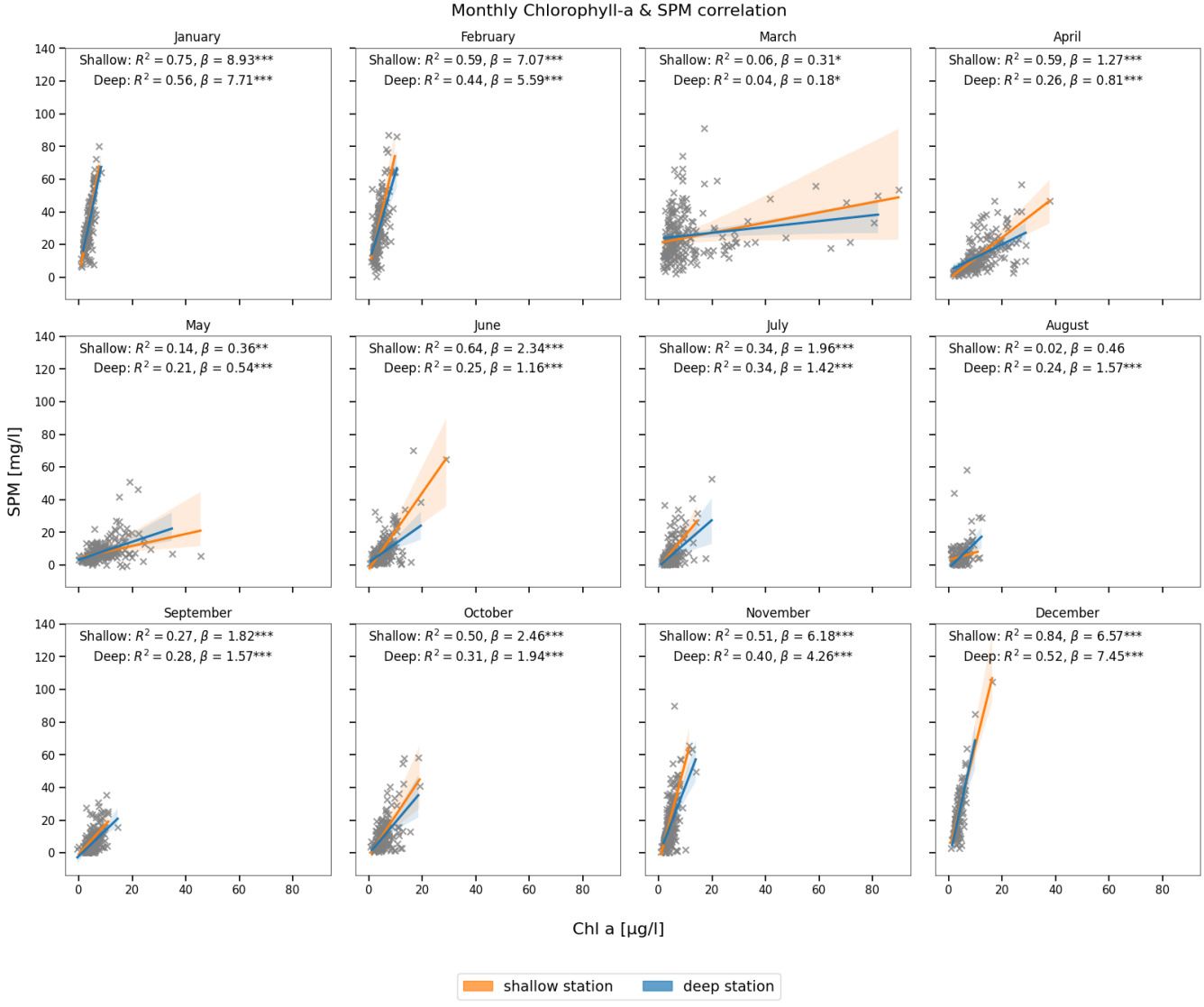


**Figure 4: Monthly correlation between Chl-a (x-axis) and SPM (y-axis) concentrations at the deep (blue) and shallow (orange) stations. The coefficient of determination ($R^2$), slope (β), and statistical significance (***p < 0.001, **p < 0.01, *p < 0.05) are indicated in each panel.**

### 3.1.2 Role of wind forcing in seasonal SPM variations

The relationship between seasonal SPM concentrations and wind characteristics is illustrated in Fig. 5. The results reveal a clear seasonal cycle in wind speed, which closely aligns with variations in SPM levels. The lowest wind speeds in summer correspond to the lowest SPM concentrations, while the increase in wind speeds in autumn coincides with rising SPM levels.
Wind speeds are highest in winter, averaging around 8.5 ± 2.8 m/s, with peaks reaching 14.2 ± 1.7 m/s in January. Through spring, they gradually decline, reaching a summer minimum with mean speeds

https://doi.org/10.5194/egusphere-2025-2135
Preprint. Discussion started: 18 June 2025


around 6.5 ± 3.1 m/s and minima of 2.0 ± 0.7 m/s in July–August. In autumn, wind speeds begin to rise again. The dominant wind direction shifts throughout the year, with a predominance of westerly (W) and northwesterly (NW) winds, except for southerly winds in late autumn (October–November) and easterly winds in April. Dominant wind directions also vary throughout the year, with westerly and northwesterly winds prevailing in most months, easterly winds in April, and more southerly winds during late autumn (October–November). However, no clear linear relationship emerges between dominant wind direction and seasonal SPM concentrations. To account for potential nonlinear interactions that may still play a role, wind direction was included as an input feature in the NN model.

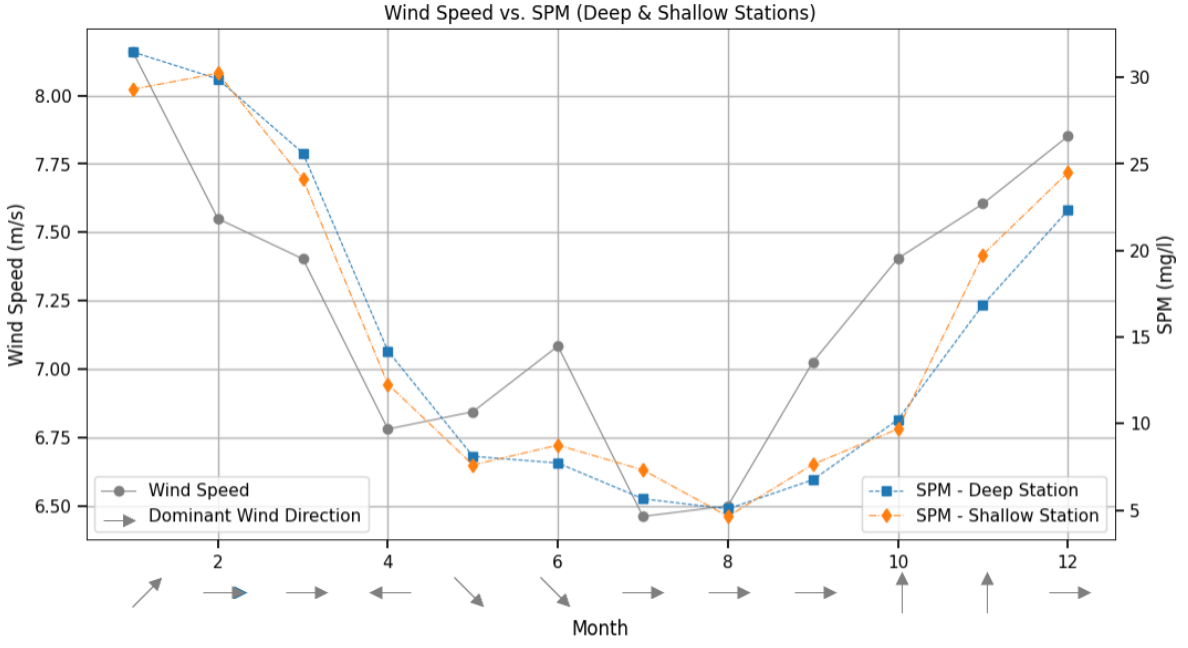


**Figure 5: Monthly averages of wind speed, SPM concentrations, and dominant wind direction (2000–2019). The figure illustrates monthly mean wind speed (grey solid line, left axis) and SPM concentrations at the deep (blue squares) and shallow (orange diamonds) stations (right axis). Grey arrows along the x-axis represent the dominant wind direction for each month, with arrow orientation indicating the direction from which the wind originates, following standard meteorological convention.**

The correlation between instantaneous wind speed and SPM is strongest in winter (Fig. 6), particularly pronounced at the shallow station, peaking in January with $R^2 = 0.44$. This suggests that wind-driven resuspension is a dominant control on SPM concentrations in winter. In contrast, the deep station shows much weaker correlations, with $R^2$ values often near zero, suggesting that the wind intensity may have a lagged effect on SPM levels.

During summer (June–August), the relationship weakens significantly, with the lowest correlations observed in August for both stations. The shallow station maintains some correlation into late summer and early autumn.

https://doi.org/10.5194/egusphere-2025-2135
Preprint. Discussion started: 18 June 2025


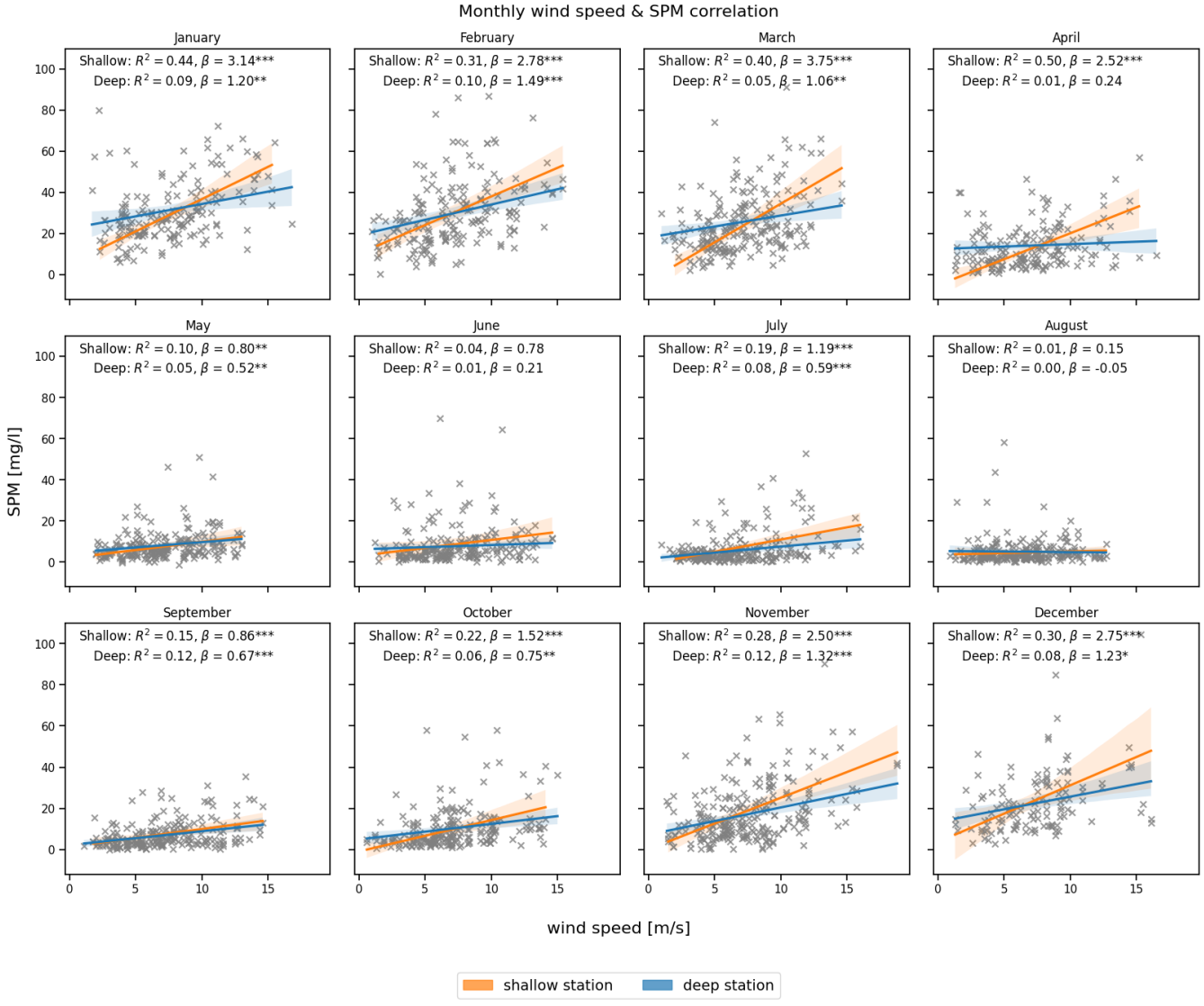


**Figure 6: Monthly correlation between wind speed at the time of sampling (x-axis) and SPM concentration (y-axis) at the deep (blue) and shallow (orange) stations. The coefficient of determination ($R^2$), slope (β), and statistical significance (***p < 0.001, **p < 0.01, *p < 0.05) are indicated in each panel.**

In contrast to the instantaneous impact of wind-speed, averaging wind speed over 120 hours (5 days) results in a stronger correlation between wind and SPM, as shown in Fig. 7, although the seasonal pattern remains similar. The stronger relationship is particularly evident in the winter and autumn months, especially at the deep station (e.g., $R^2$ = 0.35 in September, 0.24 in November and February). These findings indicate that the average wind characteristics over several days have a stronger influence on SPM levels than the wind at the time of sampling.

The results highlight that wind plays a crucial role in controlling SPM variability, particularly in shallow waters during winter and autumn. Naturally, the influence of wind is less pronounced in deeper

https://doi.org/10.5194/egusphere-2025-2135
Preprint. Discussion started: 18 June 2025


waters through direct resuspension mechanisms. However, it remains significant, with a time lag possibly caused by the transport of resuspended material from shallower zones to the deep station. This aspect is further discussed below, in Section 3.2.3.

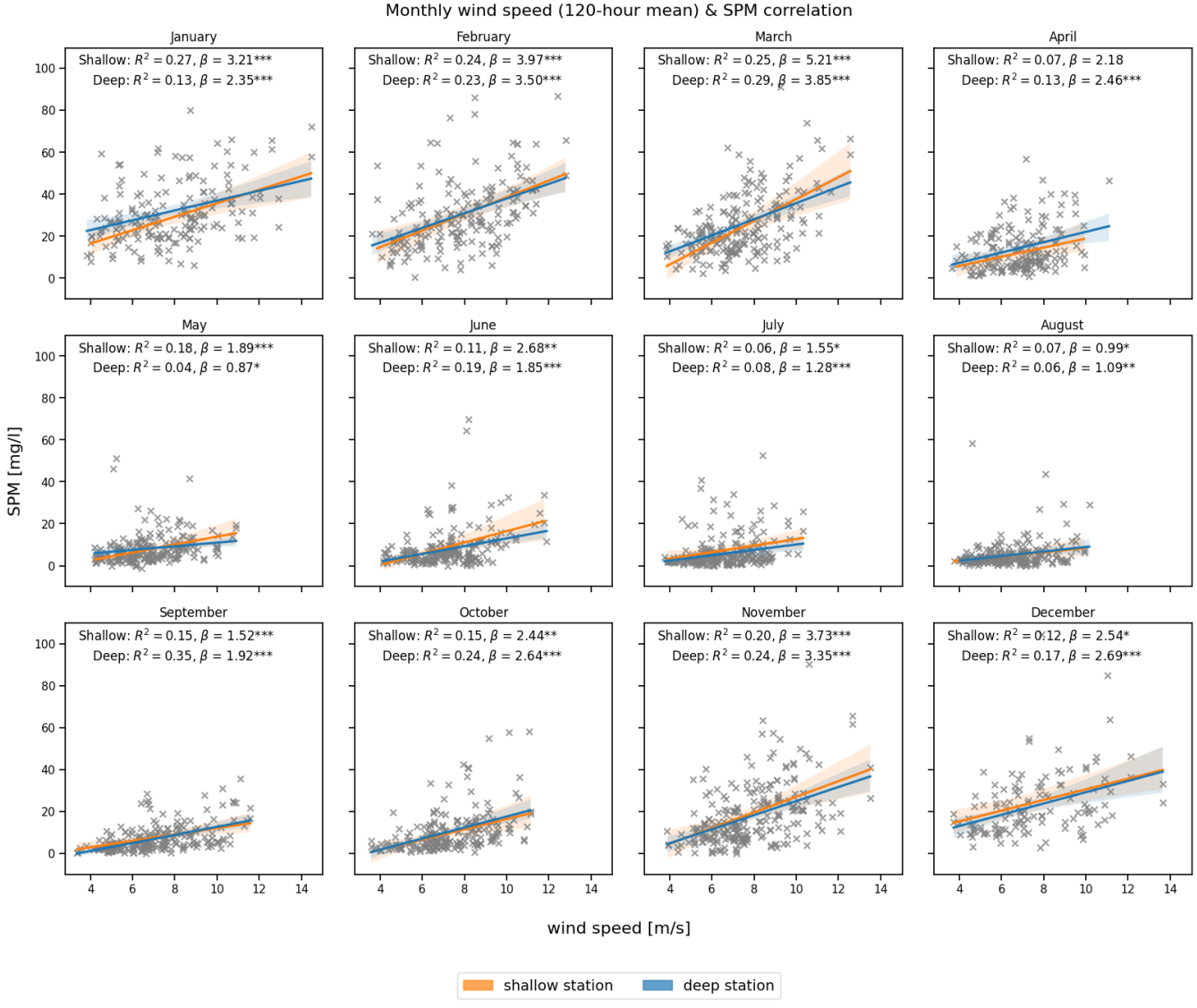


**Figure 7: Monthly correlation between wind speed averaged over a 120-hour (5-day) period (x-axis) and SPM concentration (y-axis) at the deep (blue) and shallow (orange) stations. The coefficient of determination ($R^2$), slope (β), and statistical significance (***p < 0.001, **p < 0.01, *p < 0.05) are indicated in each panel.**

## 3.2 Resuspension and Time Scales of Inner Basin Transport

In addition to factors playing a role in seasonal SPM variability, there are mechanisms responsible for SPM levels in shorter temporal scales, from hours to days. This subsection examines how wind-induced resuspension operates over different time frames and the role of tidal transport within the basin.

https://doi.org/10.5194/egusphere-2025-2135
Preprint. Discussion started: 18 June 2025


### 3.2.1 Influence of SSH

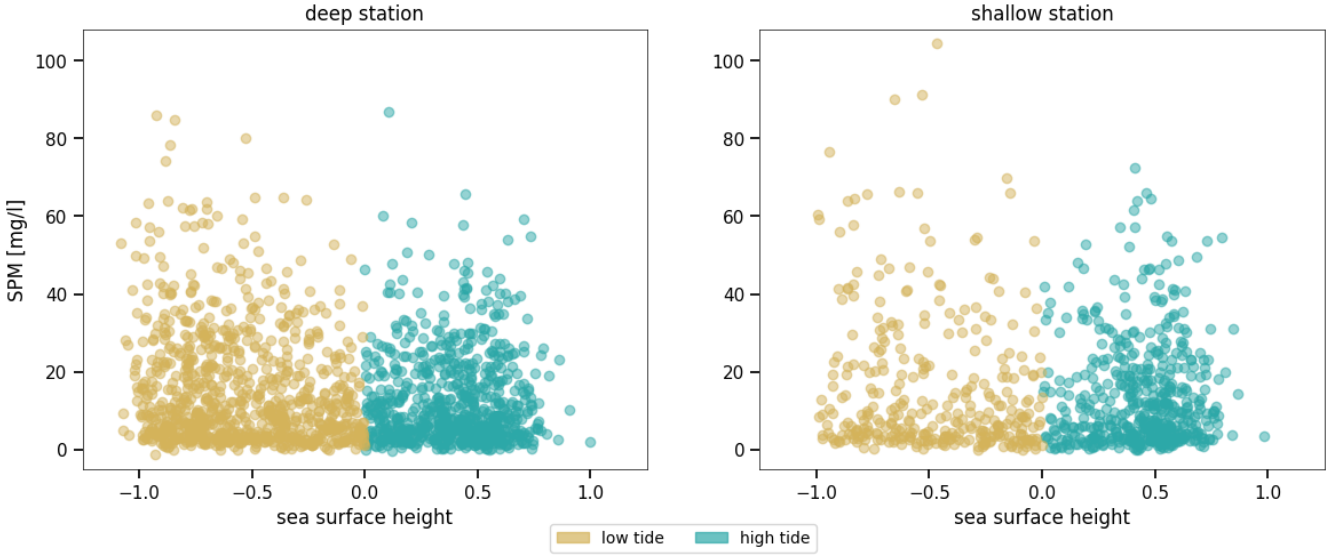


**Figure 8: SPM concentrations VS sea surface height (SSH), where SSH<0 is low tide and SSH>0 is high tide.**

SPM concentrations tend to be higher during low tide (SSH < 0) and lower during high tide (SSH > 0), as shown in Fig. 8. This relationship reflects the effect of tidal water level on sampling depth. At low tide, when the water column is shallower, the samples capture more of the resuspended particulate matter, whereas at high tide, SPM concentrations are slightly smaller with the increased water depth. This effect produces a more pronounced gradient at the shallow station, where the total water depth is around 2 meters. Here, tidal fluctuations significantly alter the vertical position of the sample relative to the seabed, making SPM concentrations more sensitive to SSH changes. In contrast, at the deeper station (~10 meters depth), this vertical shift has a smaller relative impact on the sampling position, and therefore on SPM values.

Beyond modulating sampling depth, tidal forcing itself also promotes resuspension. Due to the presence of tidal asymmetry in the area, characterized by a difference in maximum and mean velocities between flood and ebb phases, the resulting resuspension is also not entirely balanced across the tidal cycle. To capture this phase-dependent variability, the gradient of sea surface height is included as an input feature in the neural network model.

https://doi.org/10.5194/egusphere-2025-2135
Preprint. Discussion started: 18 June 2025


### 3.2.2 Role of wind forcing in short time SPM variations

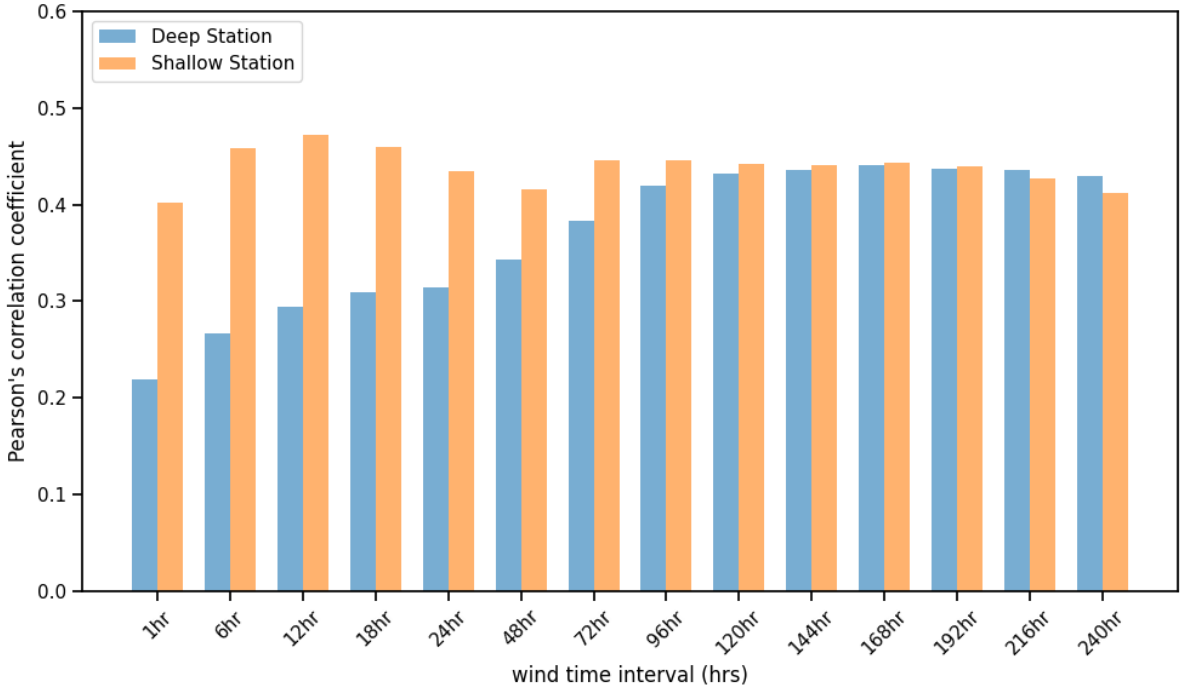


**Figure 9: Pearson correlation coefficients between SPM and wind speed averaged over different time intervals, ranging from 1 hour to 240 hours. The two stations (deep station as blue and shallow station as orange) are represented separately, showing how wind memory influences SPM variability at different depths.**

The effect of wind on SPM variability is further analyzed by assessing the correlation between SPM and wind speeds averaged over different time frames – "wind memory". Figure 9 illustrates how the strength of this relationship evolves as wind speeds are averaged over progressively longer intervals, ranging from 1 hour to 240 hours. This approach quantifies how SPM responds to the cumulative influence of past wind conditions over varying time scales. The results show that correlation coefficients generally increase as wind memory lengthens, reaching a peak around 12-18 hours at the shallow station and 120 hours at the deep station, followed by a slight decline.

During winter, the correlation between wind speed and SPM is generally higher than in summer (Fig. 10). At the shallow station, correlation values peak within the first 12–18 hours, then slightly decline for longer wind memory intervals. This suggests that in shallow waters, the wind conditions at the time of sampling have an immediate reflection at the SPM levels. At the deep station, correlations are generally lower but gradually increase with longer wind memory intervals (~120 hours), followed by a plateau, indicating that deep-water SPM reflects rather the average wind speed for a prolonged duration before the sampling.

https://doi.org/10.5194/egusphere-2025-2135
Preprint. Discussion started: 18 June 2025


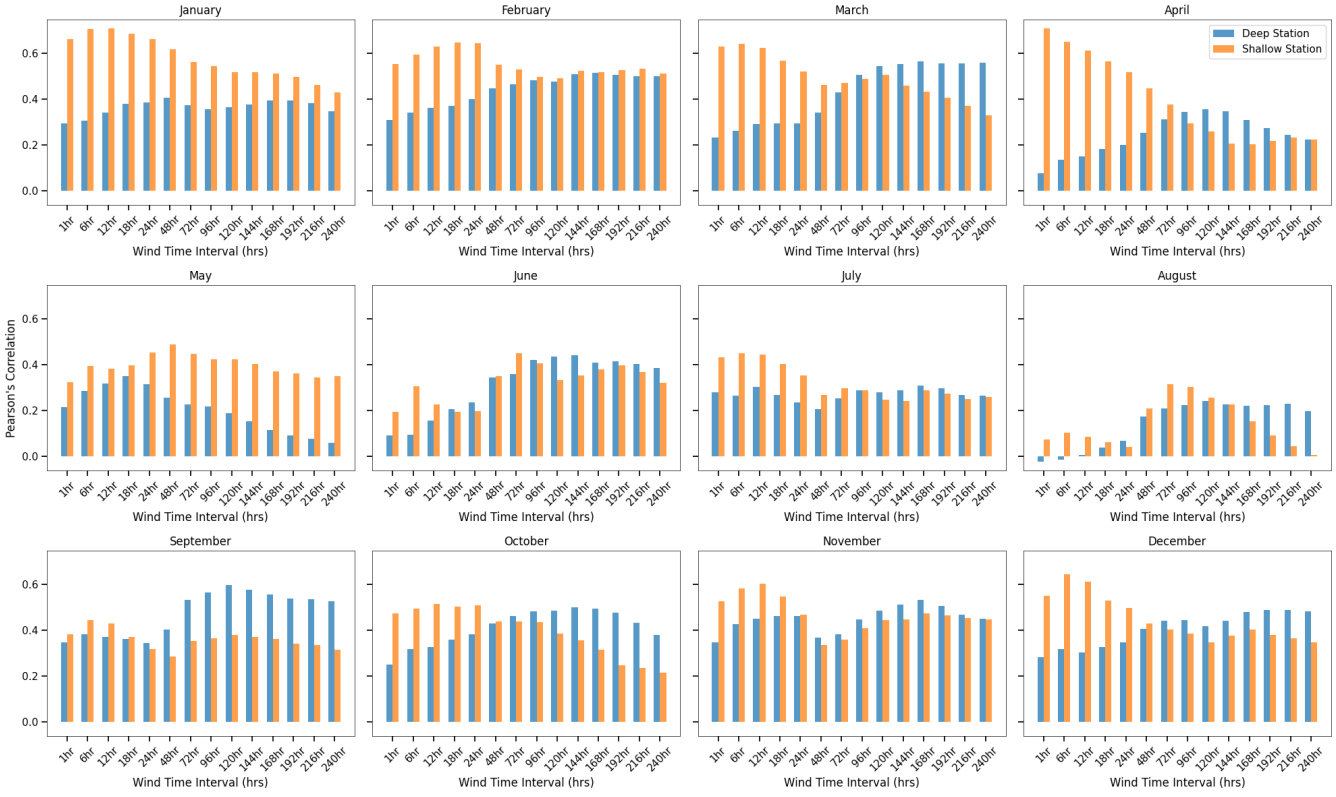


**Figure 10: This figure presents the monthly variations in the correlation between wind speed and SPM across different wind memory intervals, ranging from short-term (1 hour) to long-term (240 hours). Each panel corresponds to a specific month, displaying Pearson correlation coefficients for both the shallow and deep stations. Orange bars represent the shallow station, while the blue bars represent the deep station.**

In the spring and autumn months, the correlation patterns show more complex patterns. In April, for example, the correlation at the shallow station is highest at the time of sampling but decreases sharply as longer wind memory is considered. In contrast, months such as October and November exhibit a more gradual increase in correlation as wind memory extends.

During summer, particularly in June, July, and August, the correlation between wind speed and SPM is significantly weaker. As noted in Section 3.1.2, wind direction also shows no clear linear relationship with SPM, so this reduced summer correlation suggests that other mechanisms, beyond direct wind forcing, may be influencing SPM levels during this period. At the deep station, summer correlations remain low but increase slightly with longer wind averaging intervals, indicating that even in summer, accumulated wind forcing over multiple days can have a delayed effect on deep-water SPM.

https://doi.org/10.5194/egusphere-2025-2135
Preprint. Discussion started: 18 June 2025


### 3.2.3 Role of tidal forcing in short time SPM variations

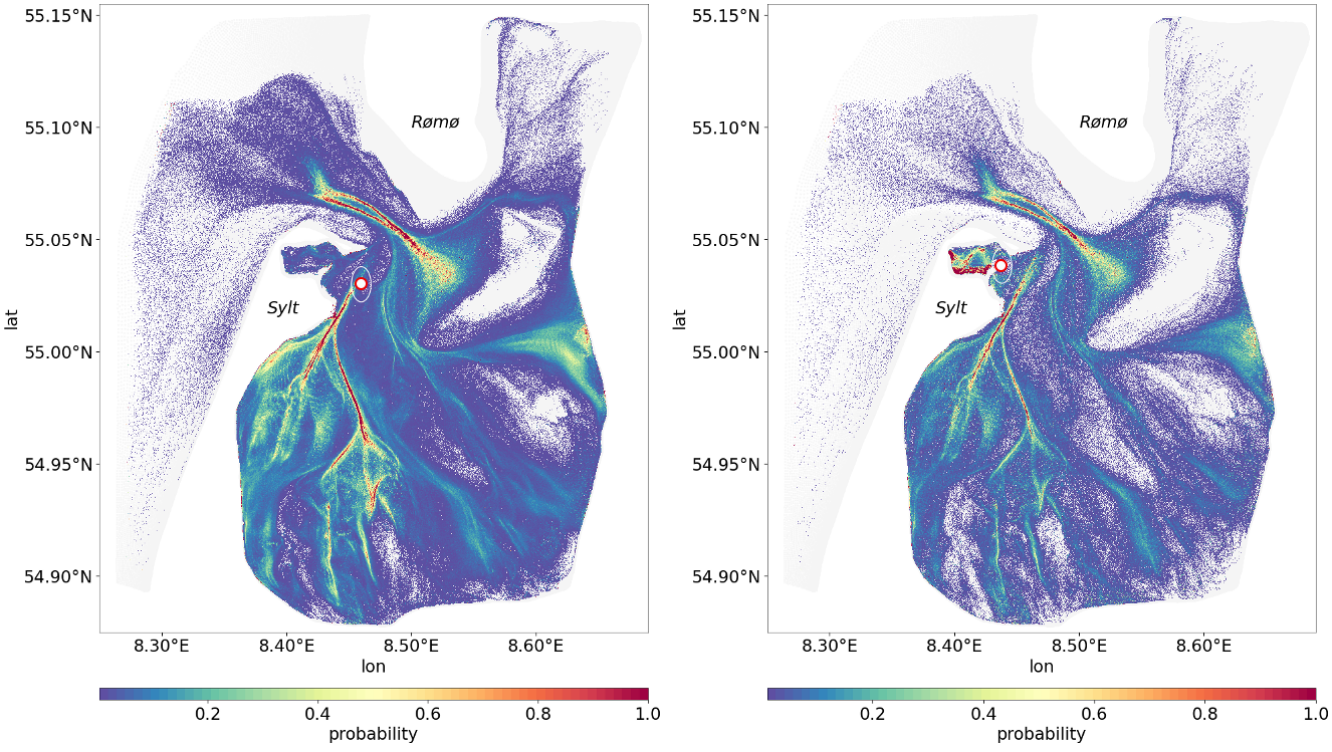


**Figure 11: Probability distribution of passive tracer pathways to illustrate how frequently different areas act as source regions or transport corridors for passive tracers. Higher probability values (highlighted in yellow and red) indicate locations that more frequently contribute to SPM reaching the deep station (left panel) or shallow station (right panel).**

Figure 11 shows the spatial probability distribution of passive tracer connectivity within the basin, derived from Lagrangian simulations forced solely by tides. This setup isolates the dominant physical driver of material transport in the Sylt-Rømø Bight, where tidal processes account for roughly 80% of velocity variability (Fofonova et al., 2019). While regular wind forcing (excluding storm events) enhances lateral dispersion through vertical mixing and stochastic fluctuations, its net contribution to basin-wide transport over tidal timescales is relatively minor (Konyssova et al., under revision). Residual currents generated by non-linear tidal interactions establish consistent, directional transport pathways, which are effectively captured by the simulated tracer trajectories.

The resulting network of tidally-induced transport pathways reveals clear differences between the two stations. Each color-coded region indicates the probability of tracers originating from that area to eventually reach the deep (left) and shallow (right) stations. Tracers were removed from the simulation upon arrival, ensuring that only pre-arrival pathways are represented; tracers that failed to reach a station within the three-week tracking window were excluded. This way, the maps highlight dominant source regions and transport pathways delivering SPM to each site. The shallow station is predominantly supplied by tracers originating in the northern parts of the bight, particularly Königshafen and its surroundings, reflecting localized and relatively rapid connections. In contrast, the

https://doi.org/10.5194/egusphere-2025-2135
Preprint. Discussion started: 18 June 2025


deep station is influenced by broader and more distributed transport pathways, integrating material from a wider area of the basin.

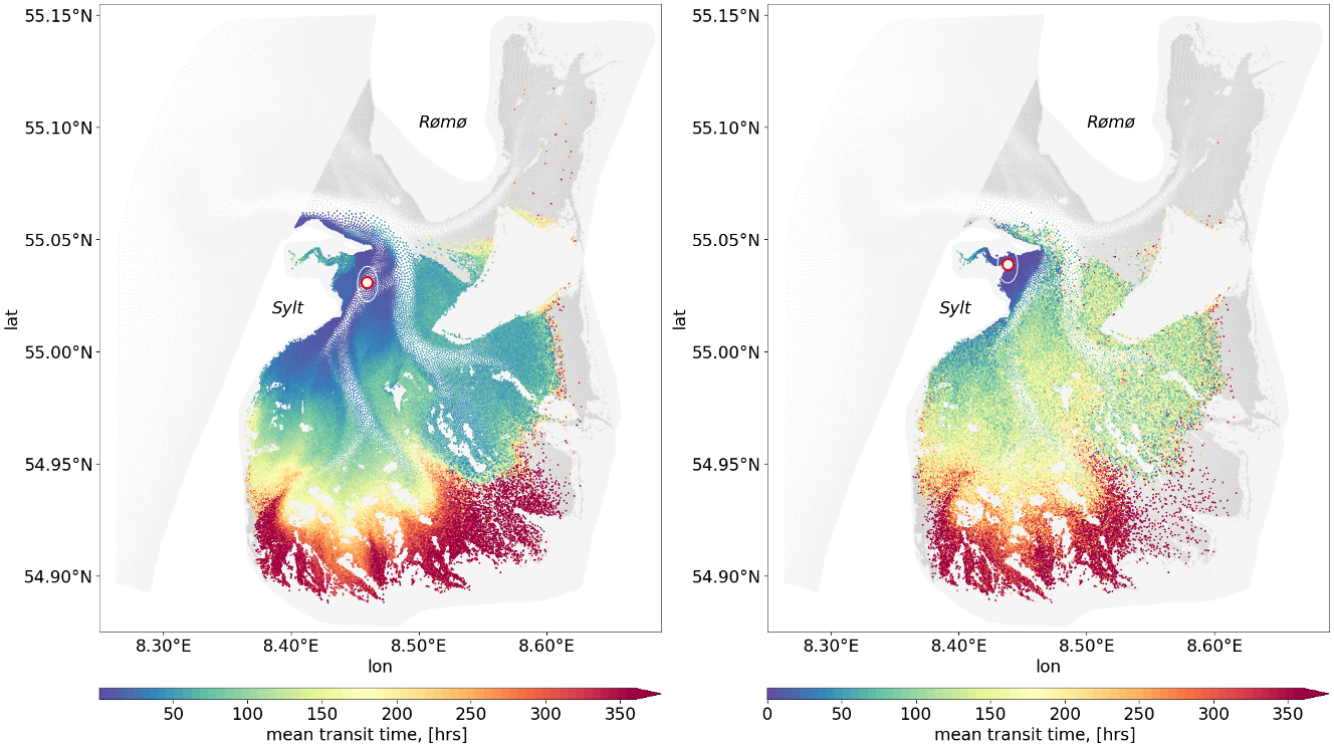


**Figure 12: The mean transit time of passive tracers to reach the sampling station. The left panel corresponds to the deep station, while the right panel represents the shallow station. Grid elements that are consistently inundated with each flood phase, from which the passive tracers are released, are shown in grey. Elements that successfully reach one of the two sampling stations are colour-coded by their mean transit time (in hours), reflecting how long it takes for passive tracers to reach from a given location to each station.**

For both stations, shorter transit times (depicted in blue and green, Fig. 12) are observed in areas closer to the stations, whereas regions further away, particularly in the inner tidal flats, exhibit longer transit times (yellow to red hues, Fig. 12). The transit time patterns reveal that SPM originating from intertidal areas and tidal channels follows particular pathways before reaching the deeper and shallower monitoring stations, with transport occurring on timescales of days to weeks. The difference between the two panels suggests that the deep and shallow stations receive material from primarily distinct but partially overlapping source regions.

Together, these figures offer a comprehensive picture of SPM transport and connectivity, showing that while both stations are influenced by tidal-driven transport, they receive material from different dominant pathways. The transit time and probability maps reveal clear differences in transport dynamics between the two sampling stations. While both stations are connected to tidal-driven transport pathways, the shallow station receives material more rapidly and from more localized sources, whereas the deep station is influenced by a broader, more distributed transport network. To quantify the typical timescale for SPM transport, a probability-weighted transit time was computed, where individual transit times were weighted according to their interpolated probability values. This approach ensures that the

https://doi.org/10.5194/egusphere-2025-2135
Preprint. Discussion started: 18 June 2025


estimated transit time reflects the most frequently occurring transport pathways rather than rare, low-probability trajectories. The resulting probability-weighted median transit time was 133.3 hours for the deep station, which aligns with the ~5-day wind-memory interval identified in Section 3.2.2, and 44.4 hours for the shallow station, highlighting the pronounced contrast in transport efficiency between the two locations. Because the shallow station is located within the potential resuspension zone, this transit time does not necessarily imply a delayed response to wind forcing. Instead, it reflects the arrival of tracers from a wider surrounding area, which slightly extends the median transit time compared to what is seen in the wind memory analysis. At the same time, the relatively short overall transit time still indicates the close proximity of the primary source region, the Königshafen embayment. In contrast, the deep station integrates SPM from more complex, multi-step transport routes over longer timescales. These transit times provide a key reference for interpreting observed SPM fluctuations at each station and may help distinguish between short-term and cumulative drivers of SPM variability.

## 3.3 Neural Network

### 3.3.1 Winter SPM prediction (Baseline Model)

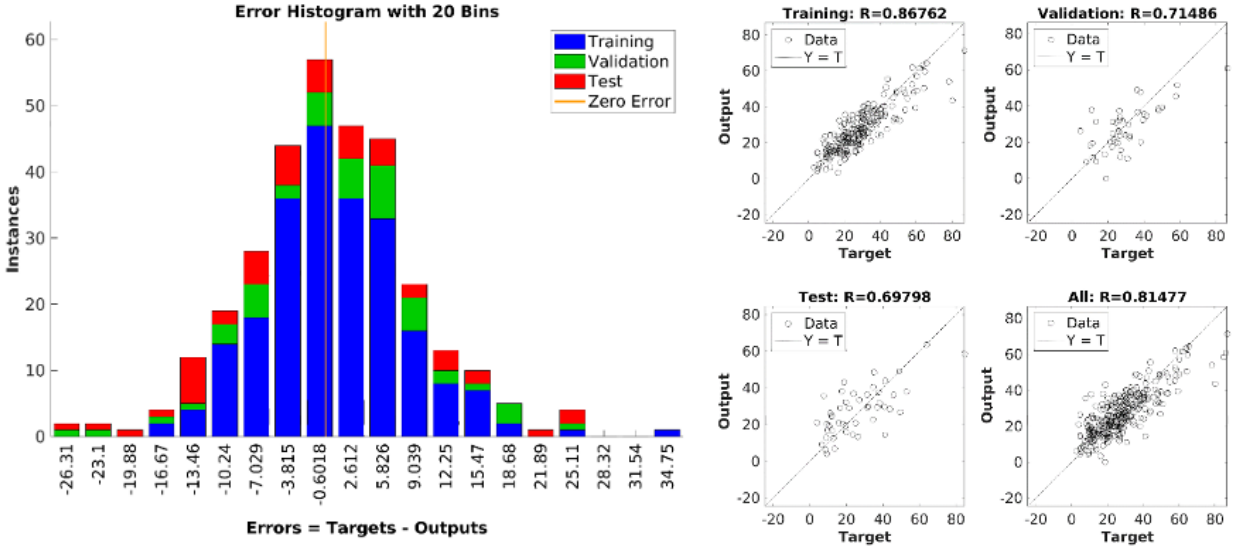


**Figure 13: Performance of the neural network (NN) trained on the winter dataset for the deep station. Left: Error histogram showing the distribution of prediction errors (in mg/L) for training, validation, and test subsets. Right: Regression plots comparing predicted vs. observed SPM values, with correlation coefficients (R) for each data subset. Due to the overall qualitative similarity between the pictures for deep and shallow stations, only the deep station is presented here.**

The error for training, validation and testing has a normal distribution (Fig. 13, left). For the deep station, the root mean square error (RMSE), a measure of average prediction error magnitude, is 9.4 mg/L for the testing set. Note that the observed mean and median SPM levels in winter are 27.6 and 25.9 mg/L respectively, as a result of the application of NN to the winter dataset, they are 27.2 and 25.5 mg/L respectively (Table 2). Regression analysis (Fig. 13, right) yields correlation coefficients between

https://doi.org/10.5194/egusphere-2025-2135
Preprint. Discussion started: 18 June 2025


observed and simulated SPMs equal to ~0.87, ~0.71, ~0.7 and ~0.81 for training, validation, testing and all winter dataset respectively.
The results show that, by using tidal and wind forcing along with a proxy for baroclinic conditions (salinity), we can predict SPM levels during winter quite well without accounting for other factors.
Next, we applied the NN trained under winter conditions to other seasons. This approach is justified by the fact that the long-term dataset captures a representative range of wind conditions in both winter and summer, including calm periods and strong wind events. Furthermore, salinity remains relatively stable across seasons, supporting the applicability of the model.
Notably, temperature, salinity, turbulent kinetic energy, and SPM levels themselves all influence flocculation processes, even without considering biological activity. Temperature was excluded from the feature set at this stage due to its strong seasonal cycle and its potential use as a proxy for biological conditions. Specifically, in our current approach, we cannot separate the influence of temperature on biological mechanisms from its physical effect (e.g. viscosity), which also impacts flocculation.

### 3.3.2 Applying of NN trained on winter data to other seasons

Using the trained winter model, we attempt to predict SPM concentrations for spring, summer, and autumn. The goal of this step is to estimate the influence of biological processes on SPM concentrations.
For both stations, the results of the NN application show significantly higher SPM levels compared to observations (Table 2).

**Table 2. Mean, median values and correlation (R) of SPM concentrations, [mg/L], from observations VS predictions by NN trained on winter dataset for the deep and shallow stations**

| seasons | | Deep Station | | Shallow Station | |
|---|---|---|---|---|---|
| | | observed | predicted | observed | predicted |
| winter | mean, [mg/L] | 27.6 | 27.2 | 28.5 | 24.7 |
| | median, [mg/L] | 25.9 | 25.5 | 24.4 | 26.5 |
| | | *R = 0.81* | | *R = 0.81* | |
| spring | mean, [mg/L] | 16.5 | 24.8 | 15.6 | 20.6 |
| | median, [mg/L] | 13.3 | 24.3 | 11.3 | 18.0 |
| | | *R = 0.29* | | *R = 0.5* | |
| summer | mean, [mg/L] | 6.15 | 17.7 | 6.8 | 18.5 |
| | median, [mg/L] | 4.22 | 16.9 | 3.9 | 16.1 |
| | | *R = 0.04* | | *R = 0.35* | |
| autumn | mean, [mg/L] | 11.6 | 23.4 | 12.8 | 24.0 |
| | median, [mg/L] | 8.5 | 22.7 | 7.5 | 21.0 |
| | | *R = 0.44* | | *R = 0.54* | |

https://doi.org/10.5194/egusphere-2025-2135
Preprint. Discussion started: 18 June 2025


.

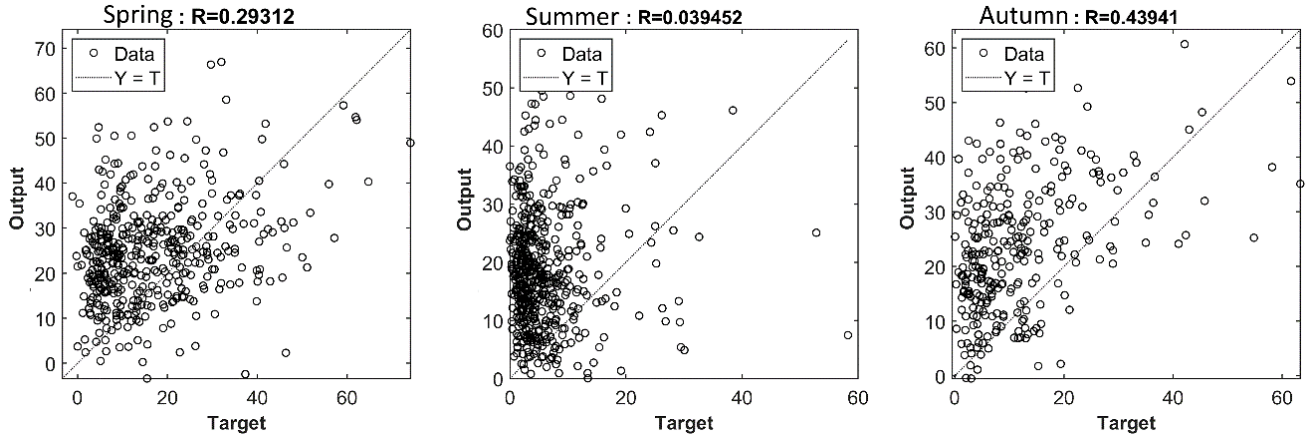


**Figure 14: Regression analysis for NN trained on winter data and applied to spring, summer and autumn data vs observations. Results shown for the deep station; shallow station results are qualitatively similar and summarized in Table 2.**

This discrepancy suggests that while calmer wind conditions alone can explain approximately 40% of the SPM reduction in summer compared to winter, they do not account for the full 80% decrease observed in the data. The overestimation of SPM by the NN is clearly visible in the regression plots (Fig. 14), where most of the predicted values are positioned above the Y = T line, particularly during summer and autumn. This does not necessarily imply that biological activity is weaker in spring, but rather that its impact is less visible due to the stronger wind conditions in spring compared to summer and autumn. The correlation coefficient between simulated and observed SPM levels in autumn is much higher than in spring, which speaks to the relatively large role of biological processes in spring compared to autumn. During summer, biological processes become the primary driver of SPM dynamics, as evidenced by the regression coefficient dropping below 0.05 (Fig. 14).

### 3.3.3 NN trained at the data from all seasons

Previously we showed that there are factors, in particular biological processes, which significantly influence the SPM dynamics. To confirm this, we trained NN on all the dataset (not only on the winter dataset) using the same 21 input features, which we used in 3.3.1.
As expected, the overall RMSE increases to approximately 11 mg/L, due to the omission of important features that influence SPM dynamics during the warm season. When trained on data from all seasons, the model is applied specifically to winter conditions, it underestimates SPM concentrations. For the deep station, the predicted mean and median are 19.17 mg/L and 17.2 mg/L, respectively, compared to observed values of 27.6 mg/L and 25.9 mg/L. At the shallow station, the model yields mean and median predictions of 20 mg/L and 17 mg/L, whereas the corresponding observed values are 28.45 mg/L and 24.35 mg/L. The regression coefficients also reflect this underperformance, with values of approximately 0.66 for the deep station and 0.72 for the shallow station.

https://doi.org/10.5194/egusphere-2025-2135
Preprint. Discussion started: 18 June 2025


### 3.3.4 NN trained at the data from all seasons and includes features that serve as proxies for biological processes

The error for training, validation and testing has a normal distribution. The RMSE for the testing is ~10 mg/L. The regression analysis shows the correlation coefficient between observed and simulated SPM levels equal to ~0.88, ~0.76, ~0.72 and ~0.84 for training, validation, testing and all datasets respectively. Supporting figures showing the error distribution and regression performance are provided in the Supplementary Material.
Notably, adding proxies for biological processes as additional features significantly improves the overall performance of the NN trained on the full dataset. When applying this enhanced NN to winter data, the correlation coefficient increases to 0.73 at the deep station and up to 0.82 at the shallow station as opposed to 0.66 and 0.72, respectively, when input features included only abiotic factors.

## 4 Discussion

This study set out to quantify the roles of tidal transport, wind-driven resuspension, and biological processes mediated by phytoplankton (e.g., direct contribution of phytoplankton biomass to SPM, biologically induced flocculation, and trophic interactions such as grazing) to SPM variability in the Sylt-Rømø Bight. Our analysis integrates long-term in-situ observations from the Sylt Roads monitoring program and Lagrangian transport analyses based on high-resolution tidal simulations using FESOM-C. The results reveal that SPM dynamics in this tidally energetic, well-mixed basin are governed by a complex interplay of physical and biological drivers that vary spatially and across different time scales. The patterns of SPM variability in the Sylt-Rømø Bight are not unique to this system but reflect more general principles of ecosystem dynamics in shallow coastal environments. Similar to other parts of the Wadden Sea, this system shows a strong seasonal cycle in SPM, with winter resuspension and summer stabilization driven by a combination of wind, tidal, and biological processes (e.g., Philippart et al., 2013). Our seasonal analysis confirmed that SPM concentrations show a pronounced seasonal cycle, with high values in winter and a decline during spring and summer. Meanwhile, Chl-a concentrations, which are used as a proxy for the phytoplankton biomass, follow an inverse seasonal pattern – low in winter and peaking during early spring. Worth noting is that this study takes Chl-a concentrations as a proxy for the phytoplankton biomass, which plays a central role in initiating biologically mediated processes, including flocculation, microbial activity and grazing.

### 4.1 Biological Interaction

The strong positive correlation between Chl-a and SPM in winter suggests that under low biological activity, such as limited phytoplankton growth, both parameters are largely driven by physical processes such as wind-driven resuspension. This is consistent with previous observations in the Wadden Sea and German Bight (van Beusekom et al., 1999; van Beusekom and de Jonge, 2002). Together with SPM, the strong winds resuspend microphytobenthos attached to sediment particles (de Jonge and van Beuseukom, 1995). In contrast, the correlation between Chl-a and SPM begins to decline in spring, despite persistent wind forcing, and reaches a minimum in summer. This seasonal decoupling suggests

https://doi.org/10.5194/egusphere-2025-2135
Preprint. Discussion started: 18 June 2025


that biological aggregation processes become increasingly dominant, promoting the formation and subsequent rapid settling of flocs following the phytoplankton bloom (Schartau et al., 2019; Maerz et al., 2016; Lunau et al., 2006). It's also worth noting that, in addition to the biological feedback, the increase in water temperature during summer also accelerates particle sinking rates by reducing water viscosity, further promoting sediment deposition (Maerz and Wirtz, 2009).

In parallel, benthic microbial processes such as biofilm formation by microphytobenthos enhance sediment stability and reduce its susceptibility to resuspension, thereby modulating the amount of SPM remaining in the water column (Andersen, 2000; Stal, 2010). Beyond microbial stabilization, benthic fauna also influences SPM dynamics through benthic-pelagic coupling. Filter-feeding benthos, such as bivalves, consume suspended particulate organic carbon (POC), effectively removing material from the water column and altering vertical fluxes of organic matter. In the Sylt-Rømø Bight, food web modelling by Baird et al. (2004) estimated that benthic consumers remove approximately 56.7 mgC $m^{-2}$ $d^{-1}$ of suspended POC – potentially a substantial fraction of total SPM, depending on the proportion of organic material within it. While robust SPM-to-POC conversion factors remain uncertain due to the unknown share of freshly formed organic matter, benthic consumption likely constitutes a significant sink for fine, organic-rich particles, particularly in areas with dense benthic communities. Although the effects of native species on bentho-pelagic coupling have been relatively well studied in the region (Baird et al., 2007), the role of introduced species remains constrained. For example, the introduction and spread of alien species such as the American razor clam (*Ensis leei*), whose abundance in the Sylt-Rømø Bight has not yet been quantified, may further amplify benthic filtration effects. In the Dutch Wadden Sea, *E. leei* has been shown to significantly alter trophic carbon flows, increasing carbon consumption by secondary producers and redirecting energy flows away from higher trophic levels (Jung et al., 2020).

### 4.2 Wind & Tide Control

The hypothesis on the role of wind forcing in controlling SPM variability is supported by our further analysis. The results suggest that the intensity of winds, rather than their dominant directions, exerts a stronger influence on the seasonal cycle of SPM. The seasonal patterns of wind speed, with maximum values in winter and minima in summer, closely mirror the trends in SPM concentrations. During summer, the weaker relationship between wind speed and SPM concentrations points to the increasing importance of biological contribution. These may include enhanced flocculation and settling of particles, increased filtration by benthic organisms, reduced sediment availability due to biological stabilization, and overall lower wind activity.

Notably, correlations between wind speed and SPM are stronger at the shallow station compared to the deep station, reinforcing the notion that shallow environments are more sensitive to wind-induced turbulence, while the effect at the deep station is observable with a certain delay.

Our analysis of wind and tidal forcing also reveals a distinction in SPM dynamics between the shallow and deep stations. At the shallow station, SPM levels closely reflect immediate wind forcing, as evidenced by the strong correlations found over short wind memory intervals (12–18 hours). This is likely due to the limited water depth, where wind-induced turbulence can quickly mobilize sediments and elevate SPM concentrations. Additionally, given the shallowness of the area around the station,

https://doi.org/10.5194/egusphere-2025-2135
Preprint. Discussion started: 18 June 2025


immediate resuspension in the vicinity of the station further reinforces this local signal. Lagrangian transport simulations further support this interpretation, though an important nuance should be clarified. For consistency, we applied the same analysis approach at both stations, however, the shallow station is itself located within the intertidal zone and receives SPM directly from resuspension at the site. The probability-weighted median transit time of about 44 hours reflects contributions from tracers released both within the Königshafen embayment, which is a primary source region, and partially from other shallow areas. While this integrated signal results in a longer median time, the actual SPM response to wind forcing at the shallow station can be nearly immediate, often occurring within one to two tidal cycles, as indicated by the short wind memory correlations. This relatively short time scale underscores the responsiveness of this station to local wind-driven processes and aligns with earlier observations in tidal flat systems, where wind effects on SPM are immediate in intertidal zones but take longer to become apparent in deeper areas (de Jonge and van Beusekom, 1995).

In contrast, the situation at the deep station is more complex. Importantly, sediment characteristics in the channels at the deep station are predominantly sandy, which typically requires stronger wind energy to be resuspended as opposed to the mud and finer material found in intertidal areas. Given these differences, our transit time calculations were focused exclusively on tracers originating from the shallow and intertidal areas, as these are the primary sources of resuspended sediment. As a result, most of the suspended material reaching the deep station is transported over longer timescales, typically within about 133 hours, through tidally modulated pathways derived from our Lagrangian simulations. This timescale is consistent with our wind memory analysis, which shows that deep-water SPM is more influenced by cumulative wind conditions over roughly five days. Together, these results highlight a clear contrast between the two stations: rapid, localized sediment response in the shallow embayment versus slower, more integrated transport processes at the relatively deep channel.

Beyond local resuspension and transport within the Sylt-Rømø Bight, tidal phases may also influence SPM concentrations through broader estuarine exchange processes. This mechanism has been described for the Dutch Wadden Sea, where high tide is associated with a greater share of North Sea water, typically lower in SPM, while low tide reflects a larger contribution from more turbid Wadden Sea water (Postma, 1981). Although not explicitly analyzed in this study, the SSH and its gradient were included as input features in the NN model to account for the potential influence of such tidal phase-modulated processes.

The spatial probability maps derived from Lagrangian simulations reveal that the northern and southern parts of the Sylt-Rømø Bight are weakly connected in terms of tracer exchange under regular tidal conditions. Passive tracers released in the northern region rarely reach either of the sampling stations, both of which are located in the southern basin. As a result, the stations, while valuable for long-term monitoring, may not fully capture the spatial variability of SPM dynamics across the entire basin, especially on shorter time scales.

### 4.3 Neural Network findings

The NN experiments provide a line of evidence supporting the seasonal shift in dominant SPM drivers independent of the statistical analysis. When trained only on winter data, where biological activity is minimal, the NN successfully captured winter SPM concentrations using solely physical parameters

https://doi.org/10.5194/egusphere-2025-2135
Preprint. Discussion started: 18 June 2025


such as wind parameters with different time intervals, salinity, and tidal elevation. At both stations, this winter model performed reasonably well ($R \approx 0.81$), confirming that physical processes alone can account for most of the observed variability during this season. However, when this model was applied to other seasons, it consistently overestimated SPM levels, especially in summer when biological activity is high and wind speed is generally weaker.

At the deep station, the observed mean SPM concentration decreased by ~78%, from 27.6 mg/L in winter to 6.2 mg/L in summer. The winter-trained NN predicted only a ~36% reduction, meaning that less than half of the observed seasonal decline could be explained by abiotic factors. Similarly, at the shallow station, observed SPM declined by 80%, while the model captured only a ~42% reduction, accounting for just over half of the change. These mismatches underscore the increasing importance of biological drivers during the summer months. Interestingly, although both stations showed similar magnitudes of overestimation, the shallow station retained higher predictive skill ($R \approx 0.35$) than the deep station ($R \approx 0.04$) in summer. This difference likely reflects the stronger and more immediate influence of wind forcing at the shallow site, where even in summer, intermittent wind events can rapidly mobilize sediments.

The addition of biologically relevant features such as temperature and sunshine duration into the full-year NN model, in Section 3.3.4, significantly improved its performance, especially at the shallow station (winter R increased to 0.82 as opposed to $R \approx 0.72$ when input features included only abiotic factors). While we do not explicitly resolve individual biological pathways, these proxies likely capture their cumulative effects as seen from the improved model fit indicating their aggregate influence is both detectable and substantial. These processes may include phytoplankton-driven aggregation and flocculation, microbial stabilization, and bentho-pelagic interactions such as benthic filtration. The potential contribution of these mechanisms is discussed in more detail in Section 4.1.

### 4.4 Study Limitations

Although, in this study, we discuss the main driving mechanisms of SPM levels in the Sylt-Rømø Bight, we also acknowledge that the system is far more complex and has more factors influencing the fluctuations of SPM levels than we investigate here. Moreover, the SPM itself is a parameter that is composed of various components and sizes in nature, and such a level of detail is not readily available in the dataset. Incorporating measurements of sediment composition (organic versus inorganic fractions) and their sizes would add more certainty into the roles of considered mechanisms modifying SPM levels. As we discussed the role of different processes, we grounded on the observed concentrations and idealised model simulations. However, the settling and resuspension processes are not directly simulated in the study. Such processes would require a different modeling framework and more detailed data, including the more accurate habitat maps and sediment grain sizes. Our Lagrangian transport simulations use massless passive tracers, which do not account for flocculation, deposition, or resuspension processes. However, despite these simplifications, the model effectively captures key patterns of spatial connectivity pathways and timescales driven by tidal dynamics.

Another limitation is the lack of direct SPM input from the open boundary. However, we hypothesise that this factor does not exhibit a strong seasonal cycle. In addition, more precise SPM predictions would benefit from neural network architectures with memory, such as Long Short-Term Memory

https://doi.org/10.5194/egusphere-2025-2135
Preprint. Discussion started: 18 June 2025


(LSTM) models, which can account for the delayed effects of biotic and abiotic conditions over several months. A North Sea–wide approach would be required to fully capture these long-term dynamics and boundary-driven influences. Within such a framework, it would also be appropriate to include additional predictors such as nutrient concentrations and benthic processes to better represent the complex interactions driving SPM variability.

While this study does not claim to offer a comprehensive representation of all the processes in play, we believe that our work presents new insights to better understand the baseline mechanisms of SPM concentration variability within the basin and across multiple timescales. As we move forward, more holistic hydro- and morphodynamic model simulations would be an interesting step to further unravel the contribution of event-based processes (extreme heat, storm events), density-driven transport, and food-web interaction.

## 5 Conclusions

This study investigated the primary drivers of SPM variability in the Sylt-Rømø Bight, a semi enclosed basin with well-mixed conditions and hydrodynamics dominantly shaped by tides. Based on long-term time-series of environmental parameters such as SPM, Chl-a, winds and light availability, in combination with Lagrangian transport simulations and application of NN methods, the analysis revealed new insights on SPM dynamics across multiple timescales and relative influence of the main driving mechanisms.

Our findings confirm that wind speed is the dominant driver of short-term SPM variability, particularly at the shallow station, where SPM concentrations respond almost immediately to wind forcing. Strong correlations between wind speed and SPM, especially during winter and autumn, indicate that resuspension in shallow waters occurs rapidly. In contrast, the deep station exhibits a more delayed response to wind forcing, with peak correlations occurring at longer wind memory intervals (~5 days). This lag reflects the fact that, at greater depths, direct resuspension due to immediate wind forcing plays a reduced role, while the transport of material from neighboring shallower areas becomes increasingly important.

Tidal dynamics primarily regulate the advection processes within the basin, redistributing fine, easily resuspendable material from shallow to the deeper areas. Lagrangian simulations illustrate that SPM at the shallow station originates locally, predominantly from within or around the Königshafen embayment. Meanwhile, at the deep station, SPM is likely supplied from the intertidal and shallow by the tidally driven redistribution over a longer timescale (~133 hours), consistent with the observed wind-memory lag (~120 hours). These results highlight the fundamental distinction between localized, wind-driven resuspension and slower, broader-scale, tide-driven transport, both of which shape SPM variability but at different spatial and temporal scales.

Seasonal analyses further emphasize the shifting balance between physical and biological controls in shaping SPM dynamics. While wind and tides dominate winter SPM variability, the onset of the spring phytoplankton bloom corresponds with a decline in SPM concentrations, likely due to biological aggregation and flocculation, leading to enhanced particle settling. The inverse seasonal patterns of Chl-a and SPM supports this interpretation, aligning with previous studies that describe the role of

https://doi.org/10.5194/egusphere-2025-2135
Preprint. Discussion started: 18 June 2025


phytoplankton in promoting flocculation and sedimentation in coastal systems. NN experiments suggest that calmer wind conditions alone can explain approximately ~40% of the observed summer SPM reduction compared to winter levels, but they do not account for up to ~80% decrease seen in the data. This substantial reduction is likely influenced by a variety of biologically related mechanisms, ranging from the microbial activity, production of EPS to zooplankton grazing. Further studies are needed to quantify the relative contributions of these individual mechanisms.
Overall, this study provides a comprehensive and quantitative assessment of how wind, tides, and biological activity interact to control SPM variability in a shallow, tidally dominated coastal system.

## Conflict of Interest

The authors declare that they have no conflict of interest.

## Author Contributions

GK performed the data analysis and wrote the initial draft of the manuscript. GK, VS, and AA carried out the numerical simulations. JvB conceptualized the study. SH, SR, IK, and KHW contributed to the discussion of methods and interpretation of the results. All authors contributed to manuscript review and editing.

## Funding

This study has been funded by the German Federal Ministry of Education and Research (BMBF) in the frame of the joint research projects MGF-Nordsee (FKZ 03F0847A), CREATE (03F0910B) and Coastal Futures (FKZ 03F0911J) part of the research mission “Protection and Sustainable use of Marine Areas”, within the German Marine Research Alliance (DAM).

## Data Availability

The source code of the FESOM-C model is publicly available via Zenodo: https://doi.org/10.5281/zenodo.2085177 (Androsov et al., 2018). The Sylt Roads observational dataset is accessible through the PANGAEA data portal: https://www.pangaea.de. Meteorological data, including hourly wind characteristics (station 3032, List auf Sylt; dataset ID: *urn:x wmo:md:de.dwd.cdc::obsgermany-climate-hourly-wind*) and daily sunshine duration (*urn:wmo:md:de-dwd-cdc:obsgermany-climate-daily-kl*), are available from the Climate Data Center (CDC) of the Deutscher Wetterdienst (DWD): https://opendata.dwd.de/climate_environment/. The Lagrangian model output and Neural Network results are available from the corresponding author upon reasonable request.

## Acknowledgements

We thank the teams involved in the Sylt Roads long-term ecological monitoring program for providing essential in-situ data. We also acknowledge the Deutscher Wetterdienst (DWD) Climate Data Center for

https://doi.org/10.5194/egusphere-2025-2135
Preprint. Discussion started: 18 June 2025


access to freely available meteorological datasets. This study was conducted as part of the research mission “Protection and Sustainable Use of Marine Areas” of the German Marine Research Alliance (DAM) and was financially supported by the German Federal Ministry of Education and Research (BMBF).

## References

Aarup, T.: Transparency of the North Sea and Baltic Sea - a Secchi depth data mining study, Oceanologia, 44, 323–337, 2002.

Andersen, T. J.: The role of fecal pellets in sediment settling at an intertidal mudflat, the Danish Wadden Sea, in: Proceedings in Marine Science, vol. 3, edited by: McAnally, W. H. and Mehta, A. J., Elsevier, 387–401, https://doi.org/10.1016/S1568-2692(00)80133-3, 2000.

Androsov, A., Fofonova, V., Kuznetsov, I., Danilov, S., Rakowsky, N., Harig, S., Holger, B., and Wiltshire, K.H.: FESOM-C, , https://doi.org/10.5281/ZENODO.2085177, 2018.

Androsov, A., Fofonova, V., Kuznetsov, I., Danilov, S., Rakowsky, N., Harig, S., Brix, H., and Wiltshire, K. H.: FESOM-C v.2: coastal dynamics on hybrid unstructured meshes, Geosci. Model Dev., 12, 1009–1028, https://doi.org/10.5194/gmd-12-1009-2019, 2019.

Baird, D., Asmus, H., and Asmus, R.: Energy flow of a boreal intertidal ecosystem, the Sylt-Rømø Bight, Mar. Ecol. Prog. Ser., 279, 45–61, https://doi.org/10.3354/meps279045, 2004.

Baird, D., Asmus, H., and Asmus, R.: Trophic dynamics of eight intertidal communities of the Sylt-Rømø Bight ecosystem, northern Wadden Sea, Mar. Ecol. Prog. Ser., 351, 25–41, https://doi.org/10.3354/meps07137, 2007.

Bale, A., Morris, A., and Howland, R.: Seasonal sediment movement in the Tamar Estuary, Oceanologica Acta, 8, 1–6, 1985.

Becherer, J., Flöser, G., Umlauf, L., and Burchard, H.: Estuarine circulation versus tidal pumping: Sediment transport in a well-mixed tidal inlet, JGR Oceans, 121, 6251–6270, https://doi.org/10.1002/2016JC011640, 2016.

van Beusekom, J. E. E. and de Jonge, V. N.: Long-term changes in Wadden Sea nutrient cycles: importance of organic matter import from the North Sea, in: Nutrients and Eutrophication in Estuaries and Coastal Waters, edited by: Orive, E., Elliott, M., and de Jonge, V. N., Springer Netherlands, Dordrecht, 185–194, https://doi.org/10.1007/978-94-017-2464-7_15, 2002.

van Beusekom, J. E. E., Brockmann, U. H., Hesse, K.-J., Hickel, W., Poremba, K., and Tillmann, U.: The importance of sediments in the transformation and turnover of nutrients and organic matter in the

https://doi.org/10.5194/egusphere-2025-2135
Preprint. Discussion started: 18 June 2025


795 Wadden Sea and German Bight, Deutsche Hydrographische Zeitschrift, 51, 245–266,
796 https://doi.org/10.1007/BF02764176, 1999.

797 Burchard, H., Flöser, G., Staneva, J. V., Badewien, T. H., and Riethmüller, R.: Impact of Density
798 Gradients on Net Sediment Transport into the Wadden Sea, Journal of Physical Oceanography, 38, 566–
799 587, https://doi.org/10.1175/2007JPO3796.1, 2008.

800 Cadée, G. C.: Increased phytoplankton primary production in the Marsdiep area (Western Dutch
801 Wadden Sea), Netherlands Journal of Sea Research, 20, 285–290, https://doi.org/10.1016/0077-
802 7579(86)90050-5, 1986.

803 Cloern, J. E.: Turbidity as a control on phytoplankton biomass and productivity in estuaries, Continental
804 Shelf Research, 7, 1367–1381, https://doi.org/10.1016/0278-4343(87)90042-2, 1987.

805 Colijn, F.: Light absorption in the waters of the Ems-Dollard estuary and its consequences for the
806 growth of phytoplankton and microphytobenthos, Netherlands Journal of Sea Research, 15, 196–216,
807 https://doi.org/10.1016/0077-7579(82)90004-7, 1982.

808 Dissanayake, D. M. P. K., Ranasinghe, R., and Roelvink, J. A.: The morphological response of large
809 tidal inlet/basin systems to relative sea level rise, Climatic Change, 113, 253–276,
810 https://doi.org/10.1007/s10584-012-0402-z, 2012.

811 Dolch, T. and Reise, K.: Long-term displacement of intertidal seagrass and mussel beds by expanding
812 large sandy bedforms in the northern Wadden Sea, Journal of Sea Research, 63, 93–101,
813 https://doi.org/10.1016/j.seares.2009.10.004, 2010.

814 Dronkers, J.: Tidal asymmetry and estuarine morphology, Netherlands Journal of Sea Research, 20,
815 117–131, https://doi.org/10.1016/0077-7579(86)90036-0, 1986.

816 Dyer, K. R.: Chapter 14 Sediment Transport Processes in Estuaries, in: Developments in
817 Sedimentology, vol. 53, Elsevier, 423–449, https://doi.org/10.1016/S0070-4571(05)80034-2, 1995.

818 Egbert, G. D. and Erofeeva, S. Y.: Efficient Inverse Modeling of Barotropic Ocean Tides, J. Atmos.
819 Oceanic Technol., 19, 183–204, https://doi.org/10.1175/1520-
820 0426(2002)019<0183:EIMOBO>2.0.CO;2, 2002.

821 Eisma, D.: Flocculation and de-flocculation of suspended matter in estuaries, Netherlands Journal of
822 Sea Research, 20, 183–199, https://doi.org/10.1016/0077-7579(86)90041-4, 1986.

823 Engel, A. and Schartau, M.: Influence of transparent exopolymer particles (TEP) on sinking velocity of
824 Nitzschia closterium aggregates, Mar. Ecol. Prog. Ser., 182, 69–76,
825 https://doi.org/10.3354/meps182069, 1999.

https://doi.org/10.5194/egusphere-2025-2135
Preprint. Discussion started: 18 June 2025


826 Fettweis, M. and Van Den Eynde, D.: The mud deposits and the high turbidity in the Belgian–Dutch
827 coastal zone, southern bight of the North Sea, Continental Shelf Research, 23, 669–691,
828 https://doi.org/10.1016/S0278-4343(03)00027-X, 2003.

829 Fettweis, M., Monbaliu, J., Baeye, M., Nechad, B., and Van Den Eynde, D.: Weather and climate
830 induced spatial variability of surface suspended particulate matter concentration in the North Sea and
831 the English Channel, Methods in Oceanography, 3–4, 25–39, https://doi.org/10.1016/j.mio.2012.11.001,
832 2012.

833 Flöser, G., Burchard, H., and Riethmüller, R.: Observational evidence for estuarine circulation in the
834 German Wadden Sea, Continental Shelf Research, 31, 1633–1639,
835 https://doi.org/10.1016/j.csr.2011.03.014, 2011.

836 Fofonova, V., Androsov, A., Sander, L., Kuznetsov, I., Amorim, F., Hass, H. C., and Wiltshire, K. H.:
837 Non-linear aspects of the tidal dynamics in the Sylt-Rømø Bight, south-eastern North Sea, Ocean Sci.,
838 15, 1761–1782, https://doi.org/10.5194/os-15-1761-2019, 2019.

839 Friedrichs, C. T. and Aubrey, D. G.: Non-linear tidal distortion in shallow well-mixed estuaries: a
840 synthesis, Estuarine, Coastal and Shelf Science, 27, 521–545, https://doi.org/10.1016/0272-
841 7714(88)90082-0, 1988.

842 Graf, G. and Rosenberg, R.: Bioresuspension and biodeposition: a review, Journal of Marine Systems,
843 11, 269–278, https://doi.org/10.1016/S0924-7963(96)00126-1, 1997.

844 Hagen, R., Winter, C., and Kösters, F.: Changes in tidal asymmetry in the German Wadden Sea, Ocean
845 Dynamics, 72, 325–340, https://doi.org/10.1007/s10236-022-01509-9, 2022.

846 Jain, A. K., Jianchang Mao, and Mohiuddin, K. M.: Artificial neural networks: a tutorial, Computer, 29,
847 31–44, https://doi.org/10.1109/2.485891, 1996.

848 de Jonge, V. N. and van Beusekom, J. E. E.: Wind- and tide-induced resuspension of sediment and
849 microphytobenthos from tidal flats in the Ems estuary, Limnol. Oceanogr., 40, 776–778,
850 https://doi.org/10.4319/lo.1995.40.4.0776, 1995.

851 Jung, A., Van Der Veer, H., Philippart, C., Waser, A., Ens, B., De Jonge, V., and Schückel, U.: Impacts
852 of macrozoobenthic invasions on a temperate coastal food web, Mar. Ecol. Prog. Ser., 653, 19–39,
853 https://doi.org/10.3354/meps13499, 2020.

854 Konyssova, G., Sidorenko, V., Androsov, A., Sander, L., Danilov, S., Rubinetti, S., Burchard, H.,
855 Winter, C., Wiltshire, K.H.: Changes in tidal dynamics in response to sea level rise in the Sylt-Rømø
856 Bight (Wadden Sea), Ocean Dynamics, https://doi.org/10.1007/s10236-025-01688-1, 2025.

Kristensen, E., Bodenbender, J., Jensen, M. H., Rennenberg, H., and Jensen, K. M.: Sulfur cycling of intertidal Wadden Sea sediments (Konigshafen, Island of Sylt, Germany): sulfate reduction and sulfur gas emission, Journal of Sea Research, 43, 93–104, https://doi.org/10.1016/S1385-1101(00)00007-1, 2000.

Kuznetsov, I., Androsov, A., Fofonova, V., Danilov, S., Rakowsky, N., Harig, S., and Wiltshire, K. H.: Evaluation and Application of Newly Designed Finite Volume Coastal Model FESOM-C, Effect of Variable Resolution in the Southeastern North Sea, Water, 12, 1412, https://doi.org/10.3390/w12051412, 2020.

Kuznetsov, I., Rabe, B., Androsov, A., Fang, Y.-C., Hoppmann, M., Quintanilla-Zurita, A., Harig, S., Tippenhauer, S., Schulz, K., Mohrholz, V., Fer, I., Fofonova, V., and Janout, M.: Dynamical reconstruction of the upper-ocean state in the central Arctic during the winter period of the MOSAiC expedition, Ocean Sci., 20, 759–777, https://doi.org/10.5194/os-20-759-2024, 2024.

Loebl, M., Dolch, T., and Van Beusekom, J. E. E.: Annual dynamics of pelagic primary production and respiration in a shallow coastal basin, Journal of Sea Research, 58, 269–282, https://doi.org/10.1016/j.seares.2007.06.003, 2007.

Lunau, M., Lemke, A., Dellwig, O., and Simon, M.: Physical and biogeochemical controls of microaggregate dynamics in a tidally affected coastal ecosystem, Limnol. Oceanogr., 51, 847–859, https://doi.org/10.4319/lo.2006.51.2.0847, 2006.

Maerz, J., Hofmeister, R., Van Der Lee, E. M., Gräwe, U., Riethmüller, R., and Wirtz, K. W.: Maximum sinking velocities of suspended particulate matter in a coastal transition zone, Biogeosciences, 13, 4863–4876, https://doi.org/10.5194/bg-13-4863-2016, 2016.

Maerz, J. and Wirtz, K.: Resolving physically and biologically driven suspended particulate matter dynamics in a tidal basin with a distribution-based model, Estuarine, Coastal and Shelf Science, 84, 128–138, https://doi.org/10.1016/j.ecss.2009.05.015, 2009.

Neder, C., Fofonova, V., Androsov, A., Kuznetsov, I., Abele, D., Falk, U., Schloss, I. R., Sahade, R., and Jerosch, K.: Modelling suspended particulate matter dynamics at an Antarctic fjord impacted by glacier melt, Journal of Marine Systems, 231, 103734, https://doi.org/10.1016/j.jmarsys.2022.103734, 2022.

Pawlowicz, R., Beardsley, B., and Lentz, S.: Classical tidal harmonic analysis including error estimates in MATLAB using T_TIDE, Computers & Geosciences, 28, 929–937, https://doi.org/10.1016/S0098-3004(02)00013-4, 2002.

Philippart, C. J. M., Salama, Mhd. S., Kromkamp, J. C., Van Der Woerd, H. J., Zuur, A. F., and Cadée, G. C.: Four decades of variability in turbidity in the western Wadden Sea as derived from corrected

Secchi disk readings, Journal of Sea Research, 82, 67–79, https://doi.org/10.1016/j.seares.2012.07.005, 2013.

Postma, H.: Sediment transport and sedimentation in the estuarine environment, American Association of Advanced Sciences, 83, 158–179, 1967.

Postma, H.: Exchange of materials between the North Sea and the Wadden Sea, Marine Geology, 40, 199–213, https://doi.org/10.1016/0025-3227(81)90050-5, 1981.

Purkiani, K., Becherer, J., Flöser, G., Gräwe, U., Mohrholz, V., Schuttelaars, H. M., and Burchard, H.: Numerical analysis of stratification and destratification processes in a tidally energetic inlet with an ebb tidal delta, J. Geophys. Res. Oceans, 120, 225–243, https://doi.org/10.1002/2014JC010325, 2015.

Reise, K. and Siebert, I.: Mass occurrence of green algae in the German Wadden Sea, Deutsche Hydrographische Zeitschrift. Supplement. Hamburg[DTSCH. HYDROGR. Z.(SUPPL.)]. 1994., 1994.

Rick, J. J., Scharfe, M., Romanova, T., Van Beusekom, J. E. E., Asmus, R., Asmus, H., Mielck, F., Kamp, A., Sieger, R., and Wiltshire, K. H.: An evaluation of long-term physical and hydrochemical measurements at the Sylt Roads Marine Observatory (1973–2019), Wadden Sea, North Sea, Earth Syst. Sci. Data, 15, 1037–1057, https://doi.org/10.5194/essd-15-1037-2023, 2023.

Schartau, M., Riethmüller, R., Flöser, G., Van Beusekom, J. E. E., Krasemann, H., Hofmeister, R., and Wirtz, K.: On the separation between inorganic and organic fractions of suspended matter in a marine coastal environment, Progress in Oceanography, 171, 231–250, https://doi.org/10.1016/j.pocean.2018.12.011, 2019.

Schubel, J. R.: Gas Bubbles and the Acoustically Impenetrable, or Turbid, Character of Some Estuarine Sediments, in: Natural Gases in Marine Sediments, edited by: Kaplan, I. R., Springer US, Boston, MA, 275–298, https://doi.org/10.1007/978-1-4684-2757-8_16, 1974.

Sidorenko, V., Rubinetti, S., Akimova, A., Pogoda, B., Androsov, A., Beng, K. C., Sell, A. F., Pineda-Metz, S. E. A., Wegner, K. M., Brand, S. C., Shama, L. N. S., Wollschläger, J., Klemm, K., Rahdarian, A., Winter, C., Badewien, T., Kuznetsov, I., Herrling, G., Laakmann, S., and Wiltshire, K. H.: Connectivity and larval drift across marine protected areas in the German bight, North Sea: Necessity of stepping stones, Journal of Sea Research, 204, 102563, https://doi.org/10.1016/j.seares.2025.102563, 2025.

Sprong, P. A. A., Fofonova, V., Wiltshire, K. H., Neuhaus, S., Ludwichowski, K. U., Käse, L., Androsov, A., and Metfies, K.: Spatial dynamics of eukaryotic microbial communities in the German Bight, Journal of Sea Research, 163, 101914, https://doi.org/10.1016/j.seares.2020.101914, 2020.

Stal, L. J.: Microphytobenthos as a biogeomorphological force in intertidal sediment stabilization, Ecological Engineering, 36, 236–245, https://doi.org/10.1016/j.ecoleng.2008.12.032, 2010.

https://doi.org/10.5194/egusphere-2025-2135
Preprint. Discussion started: 18 June 2025


923 Stanev, E. V., Schulz-Stellenfleth, J., Staneva, J., Grayek, S., Grashorn, S., Behrens, A., Koch, W., and
924 Pein, J.: Ocean forecasting for the German Bight: from regional to coastal scales, Ocean Sci., 12, 1105–
925 1136, https://doi.org/10.5194/os-12-1105-2016, 2016.

926 Wotton, R.: The Essential Role of Exopolymers (Eps) in Aquatic Systems, in: Oceanography and
927 Marine Biology, vol. 20042243, edited by: Gibson, R., Atkinson, R., and Gordon, J., CRC Press, 57–94,
928 https://doi.org/10.1201/9780203507810.ch3, 2004.